

THE PENNSYLVANIA STATE UNIVERSITY  
SCHREYER HONORS COLLEGE

DEPARTMENT OF ENGINEERING SCIENCE AND MECHANICS

EXPLORATORY STUDY OF HAFNIUM NITRIDE AND ZIRCONIUM NITRIDE  
FORMATION USING LASER-SUSTAINED PLASMA

TIMMY STRAIT

May 2012

A thesis  
submitted in partial fulfillment  
of the requirements  
for a baccalaureate degree  
in Engineering Science  
with honors in Engineering Science

Reviewed and approved\* by the following:

Judith A. Todd  
Department Head and P. B. Breneman Chair  
Professor of Engineering Science and Mechanics  
Thesis Supervisor, Chair of Committee

Joseph P. Cusumano  
Professor of Engineering Science and Mechanics  
Honors Advisor

Vladimir V. Semak  
Associate Professor of Engineering Science and Mechanics and Senior Research Associate  
Thesis Reviewer

\*Signatures are on file in the Schreyer Honors College and Engineering Science and Mechanics Office.

---

# ABSTRACT

The purpose of this thesis research was to conduct a parametric study of laser and laser plasma interactions with zirconium and hafnium metal in order to develop Zr nitride and Hf nitride coatings. The study determined optimum focal plane positions, beam power, beam speed, and gaseous atmospheric conditions to optimize the formation of a continuous nitride film on a zirconium or hafnium substrate. The use of lasers in titanium nitride formation was studied parametrically by Nassar et al. [1] and an optimal regime of titanium nitride formation was found. *Investigations of laser-sustained plasma and its role in laser nitriding of titanium* [1] was used as a starting point for this research on hafnium nitride and zirconium nitride formation. Laser-sustained plasma processing conditions for the formation of near-stoichiometric hafnium and zirconium nitrides, in an open nitrogen atmosphere, were identified.



---

# TABLE OF CONTENTS

|  | <b>Page</b> |
|--|-------------|
| <b>List of Figures</b>   | <b>iv</b>   |
| <b>Acknowledgments</b>   | <b>vii</b>  |
| <b>Chapter 1</b>   |             |
| <b>Introduction</b>  | <b>1</b>    |
| 1.1 Refractory Metals and Refractory Metal Nitrides . . . . .                | 1           |
| 1.2 The Use of Lasers in Materials Processing . . . . .                      | 1           |
| 1.2.1 The Role of a Laser-Sustained Plasma in Materials Processing . . . . . | 2           |
| <b>Chapter 2</b>   |             |
| <b>Experimental Procedure</b>  | <b>4</b>    |
| 2.1 Laser Setup and Alignment . . . . .                                      | 4           |
| 2.1.1 Mirror Alignment . . . . .   | 4           |
| 2.1.2 Lens installation . . . . .  | 4           |
| 2.2 Materials . . . . .  | 5           |
| 2.3 Sample Setup . . . . .   | 6           |
| 2.3.1 Striking a Laser-Sustained Plasma . . . . .                            | 6           |
| 2.4 Preliminary Experiments . . . . .  | 6           |
| <b>Chapter 3</b>   |             |
| <b>Results</b>   | <b>11</b>   |
| 3.1 Effect of Off-Focal Distance on Nitride Films . . . . .                  | 11          |
| 3.1.1 Hafnium Coatings . . . . .   | 11          |
| 3.1.2 Zirconium Coatings . . . . .   | 12          |
| 3.2 Effect of Laser Scan Speed on Nitride Films . . . . .                    | 13          |
| 3.3 Reproducibility of results . . . . .                                     | 15          |

|   | <b>Page</b> |
|---|-------------|
| <b>Chapter 4</b>  |             |
| <b>Discussion</b>   | <b>33</b>   |
| 4.1 Optimal Parameters for Nitride Film Production . . . . .  | 33          |
| 4.2 The Role of a Laser-Sustained Plasma in Zirconium Nitride and Hafnium Nitride<br>Production . . . . . | 34          |
| 4.3 Other Effects of the Laser Nitriding Process . . . . .  | 34          |
| <b>Chapter 5</b>  |             |
| <b>Conclusions</b>  | <b>36</b>   |
| <b>Appendix A</b>   |             |
| <b>Material Data</b>  | <b>37</b>   |
| <b>Appendix B</b>   |             |
| <b>Matlab Code</b>  | <b>41</b>   |
| <b>Bibliography</b>   | <b>43</b>   |

---

# LIST OF FIGURES

|   | Page |
|---|------|
| 1.1 The differences in methods used to produce nitride coatings: (a) the zirconium nitride coating was vaporized and deposited onto the substrate; (b) a nitrogen plasma melted the zirconium substrate and the zirconium nitride reaction occurred as the plate translated under the laser-sustained plasma. . . . .   | 2    |
| 2.1 Setup illustrating the path of the beam before entering the lasing chamber. . . .   | 5    |
| 2.2 Alumina target used for laser alignment. . . . .  | 5    |
| 2.3 Using an acrylic sheet, the focal position of the laser beam was calculated. Image (a) shows the angled acrylic resting on a peg of known height. The holes in the acrylic in (b) indicate the starting position of the laser. As the laser scanned across the acrylic, the thickness of the trail changed due to the angle of the acrylic sheet. . . . .   | 6    |
| 2.4 Top view of experimental setup for laser nitriding. . . . .   | 7    |
| 2.5 A contour plot used to determine the times that needed to be averaged. Region a) shows the spectrum data collected from the stable nitrogen plasma before it reached the hafnium substrate, region b) shows the spectrum data collected while the nitrogen plasma scanned over the hafnium substrate, and region c) shows the spectrum data collected from the nitrogen plasma after it scanned beyond the hafnium plate. . . . . | 8    |
| 2.6 Optical spectroscopy results of nitriding a hafnium plate. The red spectrum lines were from the nitrogen plasma before it began scanning over the hafnium substrate. The blue spectrum lines were collected while the nitrogen plasma scanned over the hafnium substrate. . . . .   | 9    |
| 2.7 Optical spectroscopy results of nitriding a hafnium plate. The red spectrum lines were from the nitrogen plasma before it began scanning over the hafnium substrate. The blue spectrum lines were collected while the nitrogen plasma scanned over the hafnium substrate. . . . .   | 9    |
| 2.8 Optical spectroscopy results of nitriding a zirconium plate. The red spectrum lines were from the nitrogen plasma before it began scanning over the zirconium substrate. The blue spectrum lines were collected while the nitrogen plasma scanned over the zirconium substrate. . . . .   | 10   |

|   | Page |
|---|------|
| 2.9 Optical spectroscopy results of nitriding a zirconium plate. The red spectrum lines were from the nitrogen plasma before it began scanning over the zirconium substrate. The blue spectrum lines were collected while the nitrogen plasma scanned over the zirconium substrate. . . . .                                       | 10   |
| 3.1 Varying off-focal distances on the Hf plate: (a) Laser focused on the surface of the plate; (b) Laser focused 2 mm above the surface; (c) Laser focused 4 mm above the surface; (d) Laser focused 8 mm above the surface of the plate. All scans were made at 90 mm/s. . . . .  | 12   |
| 3.2 X-Ray diffraction analysis of trail 3.1a, showing a nitride film on hafnium and the presence of oxide. . . . .  | 13   |
| 3.3 X-Ray diffraction analysis of trail 3.1b, OFD=2 mm, showing a nitride film on hafnium and more oxides. . . . .  | 14   |
| 3.4 X-Ray diffraction analysis of trail 3.1c, OFD=4 mm, showing a nitride film on hafnium with minimal oxide. . . . .   | 15   |
| 3.5 X-Ray diffraction analysis of trail 3.1d, OFD=8 mm, showing a nitride film on hafnium and no oxide present. . . . .   | 16   |
| 3.6 Varying off-focal distance on the Zr plate: (a) Laser focused on the surface of the plate; (b) Laser focused 2 mm above the surface; (c) Laser focused 4 mm above the surface; (d) Laser focused 8 mm above the surface of the plate. All scans were made at 90 mm/s. . . . .   | 16   |
| 3.7 X-Ray diffraction analysis of trail 3.6c, OFD=4 mm, showing a nitride film on zirconium with minimal oxide present. . . . .   | 17   |
| 3.8 X-Ray diffraction analysis of trail 3.6d, OFD=8 mm, showing a nitride film on zirconium with an oxide present. . . . .  | 18   |
| 3.9 ESEM image of the zirconium nitride trail, produced at an off-focal distance of 8 mm and a scan speed of 90 mm/s, at 50X magnification. . . . .   | 19   |
| 3.10 ESEM image of the zirconium nitride trail, produced at an off-focal distance of 8 mm and a scan speed of 90 mm/s, at 250X magnification. . . . .   | 20   |
| 3.11 ESEM image of the zirconium nitride trail, produced at an off-focal distance of 8 mm and a scan speed of 90 mm/s, at 2500X magnification. . . . .  | 21   |
| 3.12 A scan produced by a pre-struck laser-sustained plasma at an off-focal distance of 4 mm and a scan speed of 40 mm/s. . . . .   | 21   |
| 3.13 A cross section of a hafnium nitride scan produced at an off-focal distance of 8 mm and a scan speed of 90 mm/s. . . . .   | 22   |
| 3.14 Cross-sectional images of the samples nitrided at 8 mm off-focus and 90 mm/s: (a) using a LSP; (b) without a LSP; and (c) using 1.9 kW output power, equal to the residual laser beam passing through the LSP. Image taken from Nassar et al. [1].   | 22   |
| 3.15 The thickness of the outer edge of the hafnium nitride trail, produced at an off-focal distance of 8 mm and a scan speed of 90 mm/s, is around 250 microns. . .  | 23   |
| 3.16 The thickness of the middle of the hafnium nitride trail, produced at an off-focal distance of 8 mm and a scan speed of 90 mm/s, is around 50 microns. . . . .   | 24   |
| 3.17 The effects of nitriding with a pre-struck laser-sustained plasma compared to nitriding without a pre-struck plasma: (a) Laser focused 8 mm above surface of the plate with a pre-struck laser-sustained plasma; (b) Laser focused 8 mm above the surface without a pre-struck plasma. All scans were made at 90 mm/s. . . . | 25   |

|  | <b>Page</b> |
|--|-------------|
| 3.18 A cross section of a zirconium nitride scan produced at an off-focal distance of 8 mm and a scan speed of 90 mm/s without a pre-struck laser plasma. . . . .  | 25          |
| 3.19 A cross section of a zirconium nitride scan produced at an off-focal distance of 8 mm and a scan speed of 90 mm/s with pre-struck laser-sustained plasma. . . . .   | 26          |
| 3.20 The thickness of the outer edge of the zirconium nitride trail, produced at an off-focal distance of 8 mm and a scan speed of 90 mm/s without a pre-struck laser, plasma is around 165 microns. . . . .   | 27          |
| 3.21 The thickness of the middle of the zirconium nitride trail, produced at an off-focal distance of 8 mm and a scan speed of 90 mm/s without a pre-struck laser plasma, is around 50 microns. . . . .  | 28          |
| 3.22 The thickness of the outer edge of the zirconium nitride trail, produced at an off-focal distance of 8 mm and a scan speed of 90 mm/s with pre-struck laser-sustained plasma, is around 180 microns. . . . .  | 29          |
| 3.23 The thickness of the middle of the zirconium nitride trail, produced at an off-focal distance of 8 mm and a scan speed of 90 mm/s with pre-struck laser-sustained plasma, is around 90 microns. . . . .   | 30          |
| 3.24 CCD images of plasma extinguishing while scanning a zirconium plate at the focal point of the laser: (a) the plasma touched the edge of the zirconium plate; (b) 0.005 seconds later the plasma begins to extinguish; (c) 0.01 seconds after the plasma touched the edge of the Zr plate it extinguished. . . . .                     | 31          |
| 3.25 CCD images of a stable plasma igniting while scanning a zirconium plate at the an off-focal distance of 5mm and a translation speed of 90 mm/s: (a) the laser beam touched the edge of the zirconium plate; (b) 0.005 seconds later the plasma begins to ignite; (c) 0.005 seconds after the plasma ignited it appeared to be stable. | 32          |
| 3.26 Two scans performed on separate Zr plates on different days with the same input parameters. . . . .   | 32          |
| 4.1 A plot of scan speed versus OFD, showing regions of hafnium nitride and oxidized coating formation. . . . .  | 34          |
| 4.2 A plot of scan speed versus OFD, identifying regions of zirconium nitride and zirconium oxide formation. . . . .   | 35          |
| A.1 The material data sheet from Fine Metals Corp. detailing the purity of the samples used in this research. Page 1 of 3 . . . . .  | 38          |
| A.2 The material data sheet from Fine Metals Corp. detailing the purity of the samples used in this research. Page 2 of 3 . . . . .  | 39          |
| A.3 The material data sheet from Fine Metals Corp. detailing the purity of the samples used in this research. Page 3 of 3 . . . . .  | 40          |
| B.1 Matlab Code used to produce XRD lines. . . . .   | 41          |
| B.2 Matlab Code used to produce averaged spectrum data. . . . .  | 42          |

---

# ACKNOWLEDGMENTS

I would like to acknowledge the following:

1. Abdalla Nassar for guiding me through the many techniques that were used to perform this research, teaching me laser fundamentals and training me on laser operation, providing me with literature that started my research, and answering the many questions that I had about this research.
2. Amber Black for training me on metallography and for introducing me to L<sup>A</sup>T<sub>E</sub>X.
3. Nichole M. Wonderling for collecting XRD data.
4. Scott Kralik for training me on ESEM operation.

This research was supported by the Office of Naval Research. I would also like to acknowledge the Schreyer Honors College for their financial contribution.

I would also like to acknowledge the Department of Engineering Science and Mechanics for helping me build a sound foundation on the principles of engineering and science and for providing me with the tools to become a life-long learner.

I am especially thankful for being able to work with Dr. Judith Todd. Your guidance and support has shaped my academic career and I look forward to completing my masters research under your supervision.

---

---

# CHAPTER 1

---

## INTRODUCTION

### 1.1 Refractory Metals and Refractory Metal Nitrides

Nitride coatings can be used in a variety of applications. Nitride coatings can increase the lifetime of cutting tools because they are corrosion and wear-resistant [2]. They are chemically stable at room temperature and are only slowly degraded by strong concentrations of acids [3]. Many medical devices, such as cardiac stents, benefit from zirconium nitride coatings because the coatings are biocompatible and blood compatible [4]. Five types of nitrides form and their categories can be characterized by their electronic bonding structures. The first type is interstitial nitrides and for the purpose of this research, interstitial nitrides are the most useful type. The other four types are covalent nitrides, intermediate nitrides, salt-like nitrides, and molecule forming volatile nitrides [5]. Only eight elements form interstitial nitrides (titanium, zirconium, hafnium, vanadium, niobium, tantalum, molybdenum, and tungsten) and out of these eight, only six are refractory nitrides (titanium, zirconium, hafnium, vanadium, niobium, and tantalum). Refractory defines a material with a high degree of chemical stability and a melting temperature above 1800° C [5]. Hafnium nitride and zirconium nitride are both refractory and interstitial. Since the nitrogen atoms can rest within the metal lattice, zirconium nitride and hafnium nitride exhibit the properties of high thermal conductivity and electrical conductivity. These valuable material characteristics of hafnium nitride and zirconium nitride in addition to their hardness, wear and corrosion resistant properties, make them candidates for laser nitriding research.

### 1.2 The Use of Lasers in Materials Processing

Physical vapor deposition (PVD) and chemical vapor deposition (CVD) are the current methods of widely producing zirconium nitride and hafnium nitride coatings [6, 7]. These processes are

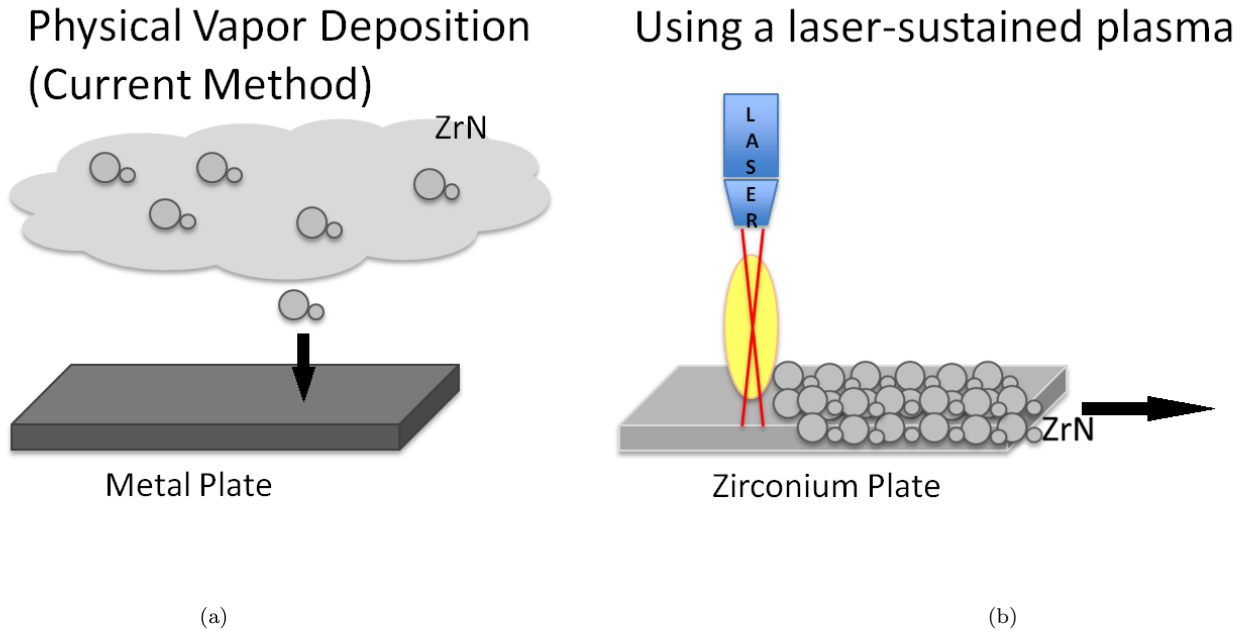


Figure 1.1: The differences in methods used to produce nitride coatings: (a) the zirconium nitride coating was vaporized and deposited onto the substrate; (b) a nitrogen plasma melted the zirconium substrate and the zirconium nitride reaction occurred as the plate translated under the laser-sustained plasma.

time consuming because the coatings are deposited in a vacuum. An illustration of this process can be seen in figure 1.1a. Because of the nature of the PVD and CVD process, the nitride coatings formed are usually on the order of microns [7]. The use of lasers in nitride processing leads to the potential for forming a continuous coating directly on a substrate [8]. This process is described in figure 1.1b. The use of lasers in nitride formation can also lead to thicker coatings on the order of hundreds of microns [9]. Preliminary experiments have characterized the effect of lasers on titanium, zirconium, and hafnium nitride coatings, respectively [10]. In previous studies a laser power equal to or less than 2 kilowatts was used and the role of a laser plasma was not well understood [2, 11].

### 1.2.1 The Role of a Laser-Sustained Plasma in Materials Processing

A laser-sustained plasma is produced when free electrons from an evaporating substrate collide with gas molecules. The excited plasma then evaporates more of the substrate causing more free electrons to be released and the process continues and is sustained by the laser power. The role of a plasma in material processing is an important one. Some argue that the laser plasma absorbs power, therefore less power reaches the substrate, while others argue that in the case of an infrared laser beam the reflected beam power can be absorbed by the laser-sustained plasma then returned back into the system [12]. Some of these theories have been tested and some



disproved. Nassar et al. [1] showed that the energy input into a substrate is not attenuated by a nitrogen laser-sustained plasma. There is also the possibility that the presence of a nitrogen-rich plasma near a metal surface will prevent an oxide from forming during the nitriding process [1]. Nassar et al. [1] have shown that the existence of a pre-struck laser-sustained plasma can also offer a larger nitriding regime than previously discovered. The research performed in this thesis investigated the hypothesis that laser-sustained nitrogen plasma can be used to develop near-stoichiometric coatings of zirconium nitride and hafnium nitride in open atmosphere.

---

---

## CHAPTER 2

---

# EXPERIMENTAL PROCEDURE

### 2.1 Laser Setup and Alignment

#### 2.1.1 Mirror Alignment

Laser alignment is important in order to maximize the laser power reaching the substrate. The laser used for this research was a 5 kW PRC Laser Corp. STS5000 CO<sub>2</sub> laser. During the experiments, the laser was operating at an output power of approximately 3.5 kW. The laser and mirror setup is illustrated in figure 2.1. The mirrors were oriented to direct the beam into the chamber such that the beam was normal to the lens. Each mirror was adjusted separately and in small increments, starting with the mirror closest to the laser output port. Ideally the laser beam should be at the center of each mirror. After an adjustment was made, a test burn was made onto an alumina target. The cross hairs on the target determined whether the mirror needed further adjustment. An example of such a target can be found in figure 2.2. Within the chamber, the CO<sub>2</sub> beam was focused using a 2 inch diameter, 5 inch focal length, ZnSe lens which was housed in a Precitec, Inc. CM2" (Z) laser cutting head.

#### 2.1.2 Lens installation

After the installation of a new lens, the focal plane position with respect to the three-axis stage was calculated. This enabled the laser operator to accurately input stage commands regarding the off-focal distance of the laser. The setup for determining the focal position is illustrated in figure 2.3a. As shown in figure 2.3a, the stage moved from right to left as the position of the laser remained constant. The focal position of the laser beam was identified in the acrylic burn at the point where the laser beam produced the smallest cut in figure 2.3b and the corresponding height was calculated using trigonometry and the geometry of the acrylic sheet in figure 2.3a.

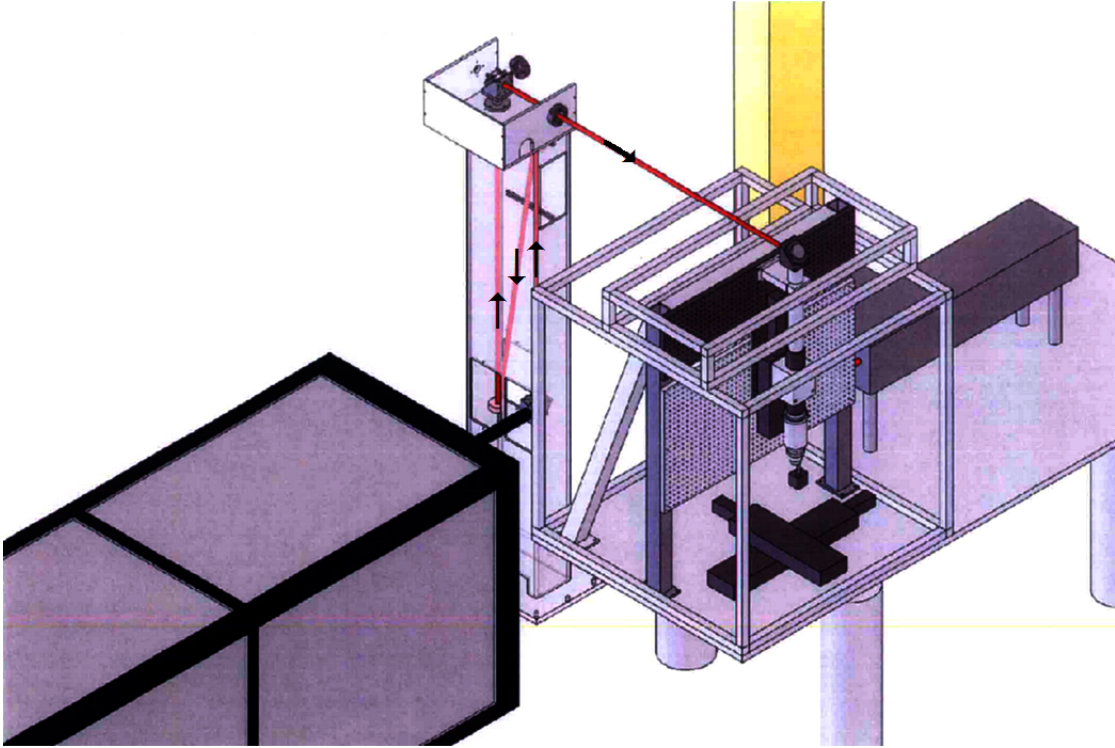


Figure 2.1: Setup illustrating the path of the beam before entering the lasing chamber.



Figure 2.2: Alumina target used for laser alignment.

## 2.2 Materials

The materials used in this study were hafnium and zirconium. The hafnium was 99.95% pure and the zirconium 702 was 99.8% pure. A detailed analysis of the materials can be found in appendix A. Refractory metals such as hafnium or zirconium are expensive compared to metals such as steel or titanium.

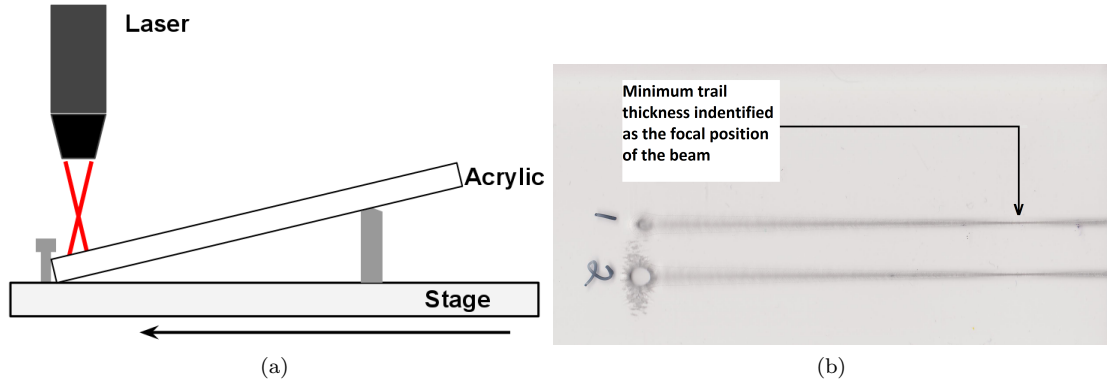


Figure 2.3: Using an acrylic sheet, the focal position of the laser beam was calculated. Image (a) shows the angled acrylic resting on a peg of known height. The holes in the acrylic in (b) indicate the starting position of the laser. As the laser scanned across the acrylic, the thickness of the trail changed due to the angle of the acrylic sheet.

## 2.3 Sample Setup

The parameters tested were off-focal distance and scan speed. The laser scans were spaced such that there were no overlaps of the processed trails. All samples were cleaned with acetone to remove any contaminants. Figure 2.4 illustrates the setup of the sample on the stage. A three-axis stage was controlled via a LabView program which varied the off-focal distance of the laser, stage position, and translation speed.

### 2.3.1 Striking a Laser-Sustained Plasma

A titanium plate was used to ignite the laser-sustained plasma (LSP) prior to scanning the plate under the pre-struck LSP. Power measurements were recorded on each day of the experiments

## 2.4 Preliminary Experiments

A charge-coupled device (CCD) was used to record the laser nitriding process. However, appropriate wavelength filters were needed to view nitrogen species in the plasma or substrate emissions during laser processing. To determine the appropriate wavelength filters, optical spectroscopy was performed on hafnium and zirconium during processing. The hafnium and zirconium plates were processed with a nitrogen laser-sustained plasma (LSP) normal to the surface of each plate. A titanium plate was used to ignite the LSP. The translation speed of each of the Hf and Zr plates was 75 mm/s. The laser was focused above the surface of the plates. The Hf plate and the Zr plate were both cleaned with acetone prior to processing. Data were collected at a 4 ms integration time using an Ocean Optics spectrometer. Since the collected data consisted of spectra that changed over the processing time, the data were analyzed using Matlab. A contour plot was generated to determine the spectrum that corresponded to a specific processing step. As

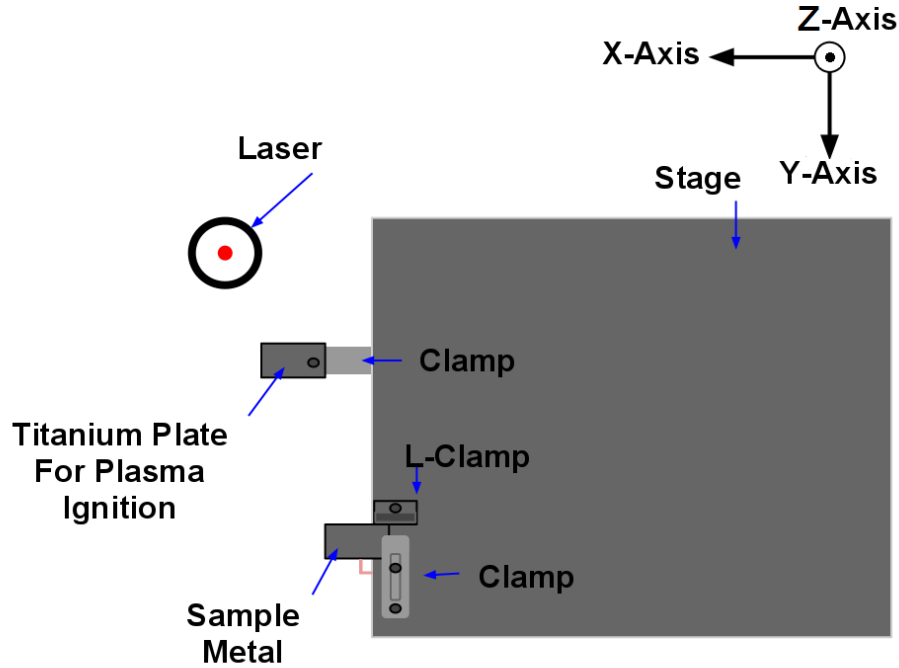


Figure 2.4: Top view of experimental setup for laser nitriding.

shown in figure 2.5, when the nitrogen plasma was ignited and stabilized, it emitted the spectrum shown in figure 2.5a. As the nitrogen plasma scanned over the substrate, the spectrum shown in figure 2.5b was generated. The spectral data, consisting of only stabilized nitrogen plasma were averaged to obtain a single spectrum. The spectra collected as the nitrogen plasma scanned over the substrate were also averaged to obtain a single spectrum. The Matlab code used to average the data is presented in appendix B. The optical spectroscopy results from the Hf plate are shown in figures 2.6 and 2.7. Figures 2.6 and 2.7 show the spectrum of the nitrogen plasma in red. The blue spectra in figures 2.6 and 2.7 was the spectra of hafnium and nitrogen plasma as the LSP scanned across the Hf plate. A closer look at figure 2.6 shows that as the LSP translated over the hafnium plate near 870 nm, the same peaks appeared. This showed that a band pass filter can be used in this region to detect only the nitrogen LSP and not the hafnium wavelength emissions. A closer look at figure 2.7 showed that the nitrogen plasma had a low intensity but the LSP scan across the hafnium plate produced intense peaks around 724 nm. This showed that a band pass filter of 720 nm could be used to detect hafnium emissions. In figures 2.6 and 2.7, a 0.6 neutral density (ND) filter was used in the collection of the hafnium spectroscopy data. The optical emission spectroscopy results for the Zr plate are shown in figures 2.8 and 2.9. Figures 2.8 and 2.9 show the spectrum of the nitrogen plasma in red. The nitrogen and zirconium spectra were collected using a 0.6 ND filter to limit the intensity of the spectra. The blue spectrum in figures 2.8 and 2.9 show zirconium and nitrogen plasma as the LSP scanned across the Zr plate. A closer look at figure 2.8 showed that, as the LSP translated over the zirconium plate near

820 nm, the same peaks appeared. Therefore, a band pass filter could be used in this region to detect only the LSP and not the zirconium wavelength emissions. A closer look at figure 2.9 showed that the nitrogen plasma had a low intensity but the LSP scan across the zirconium plate produced intense peaks around 710 nm. As a result, a band pass filter of 710 nm could be used to detect zirconium emissions while filtering out the nitrogen plasma emissions.

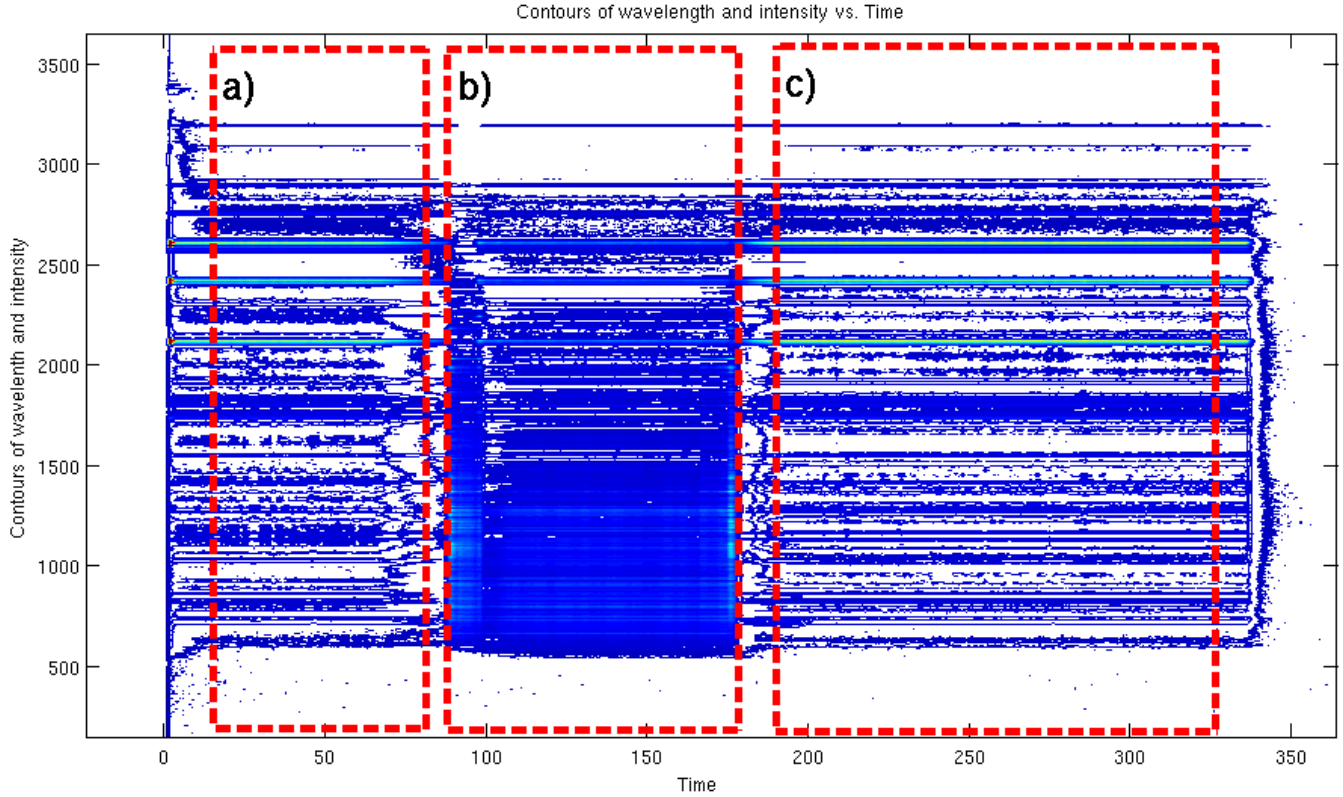


Figure 2.5: A contour plot used to determine the times that needed to be averaged. Region a) shows the spectrum data collected from the stable nitrogen plasma before it reached the hafnium substrate, region b) shows the spectrum data collected while the nitrogen plasma scanned over the hafnium substrate, and region c) shows the spectrum data collected from the nitrogen plasma after it scanned beyond the hafnium plate.

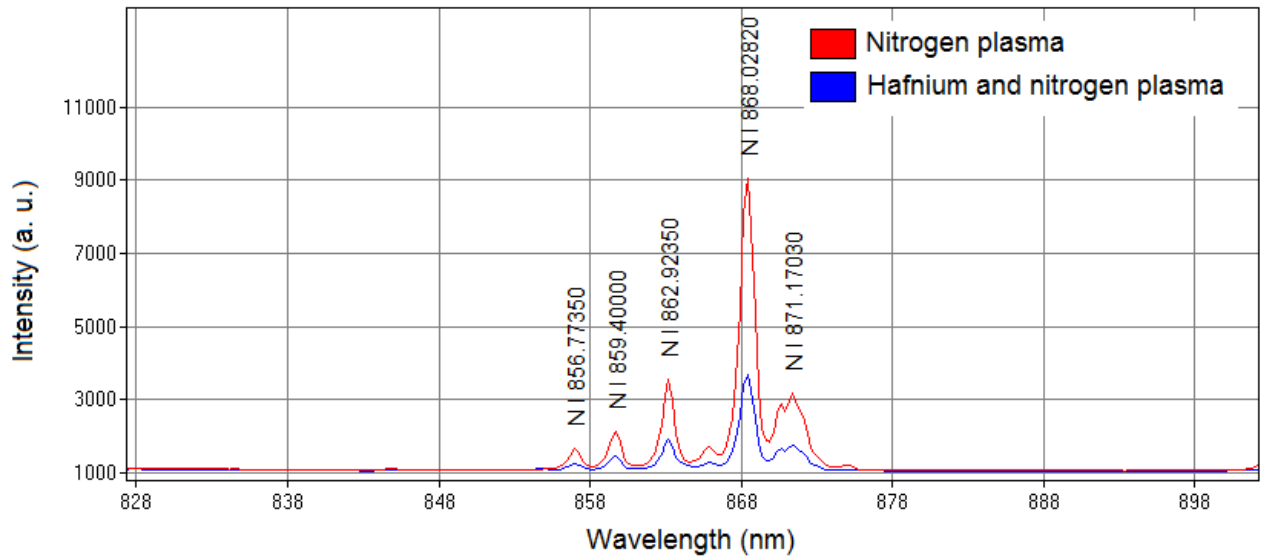


Figure 2.6: Optical spectroscopy results of nitriding a hafnium plate. The red spectrum lines were from the nitrogen plasma before it began scanning over the hafnium substrate. The blue spectrum lines were collected while the nitrogen plasma scanned over the hafnium substrate.

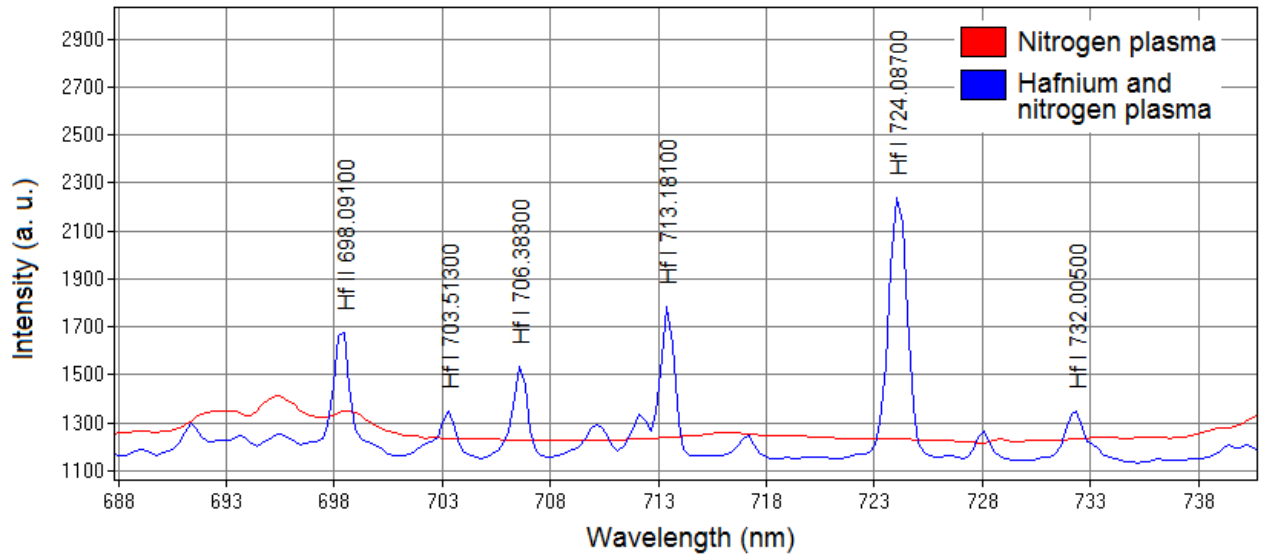


Figure 2.7: Optical spectroscopy results of nitriding a hafnium plate. The red spectrum lines were from the nitrogen plasma before it began scanning over the hafnium substrate. The blue spectrum lines were collected while the nitrogen plasma scanned over the hafnium substrate.

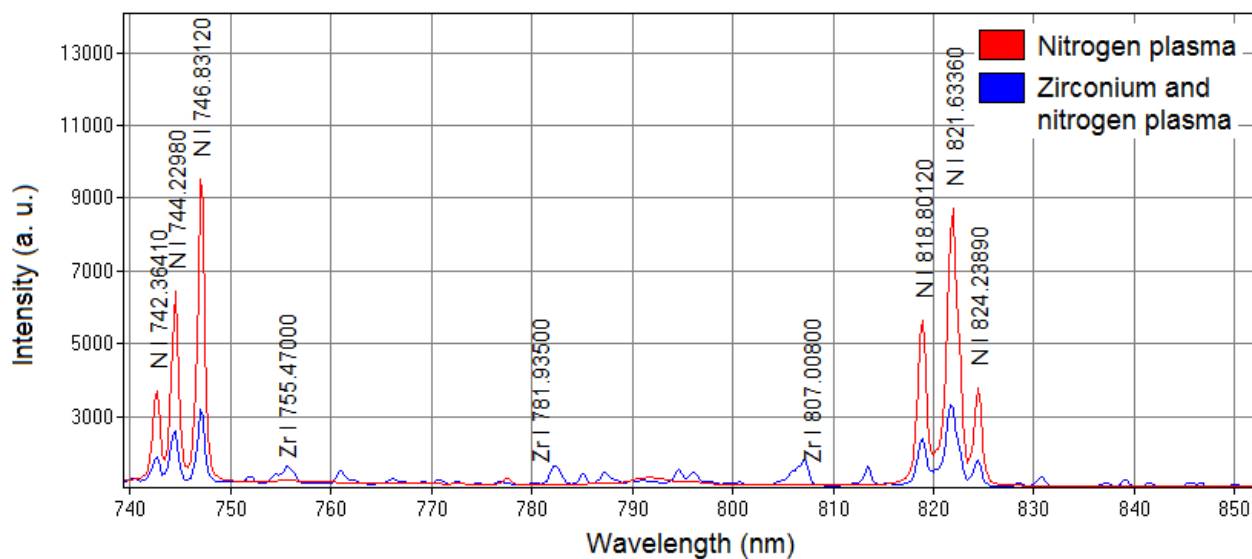


Figure 2.8: Optical spectroscopy results of nitriding a zirconium plate. The red spectrum lines were from the nitrogen plasma before it began scanning over the zirconium substrate. The blue spectrum lines were collected while the nitrogen plasma scanned over the zirconium substrate.

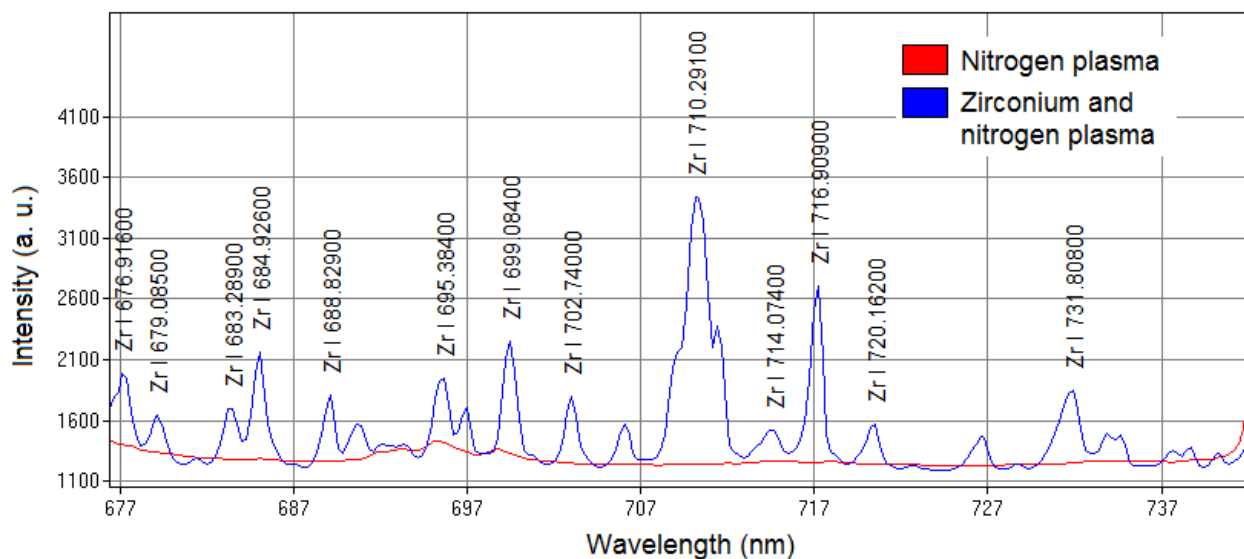


Figure 2.9: Optical spectroscopy results of nitriding a zirconium plate. The red spectrum lines were from the nitrogen plasma before it began scanning over the zirconium substrate. The blue spectrum lines were collected while the nitrogen plasma scanned over the zirconium substrate.



---

---

# CHAPTER 3

---

## RESULTS

### 3.1 Effect of Off-Focal Distance on Nitride Films

Hafnium (Hf) and zirconium (Zr) plates were processed with a pre-struck nitrogen laser-sustained plasma (LSP) normal to the surface. In each case, the plate was translated under the LSP at a speed of 90 mm/s. Off-focal distances (OFD) of 0 mm, 2 mm, 4 mm, and 8 mm were investigated. The Hf plate and the Zr plate were both cleaned with acetone prior to processing.

#### 3.1.1 Hafnium Coatings

The colors of hafnium nitride range from a pale yellow for lower nitrogen concentrations to a bright golden color for near-stoichiometric nitrogen concentrations [6]. As shown in figure 3.1, scans 3.1a and 3.1b are mostly gray with traces of a golden color. XRD results of scans 3.1a and 3.1b shown in figures 3.2 and 3.3, respectively, indicate predominately hafnium metal with some nitrides and a small amount of oxide present. XRD results of scan 3.1c, shown in figure 3.4 indicate a mixture of hafnium nitride, hafnium oxide, and hafnium metal. XRD results of scan 3.1d, shown in figure 3.5 show strong hafnium nitride peaks and minimal oxide. Although the purple and green color of scan 3.1d would indicate the presence of an oxide, XRD analyses indicated minimal hafnium oxide. Scans 3.1a and 3.1b were both noticeably rough and irregular compared to scans 3.1c and 3.1d. Scan 3.1d was the most consistent and smooth scan. The XRD analyses were performed with a PANalytical XPert Pro MPD theta-theta Diffractometer. The large peaks at 40 degrees in figures 3.2a, 3.3a, 3.5a, and 3.4a were identified as hafnium nitride in all cases. The results from figure 3.5a indicate that an off-focal distance of 8 mm will produce greater amounts of hafnium nitride at a translation speed of 90 mm/s, than smaller off-focal distances.

After the hafnium nitride results were analyzed, similar experiments to characterize zirconium nitride were performed.

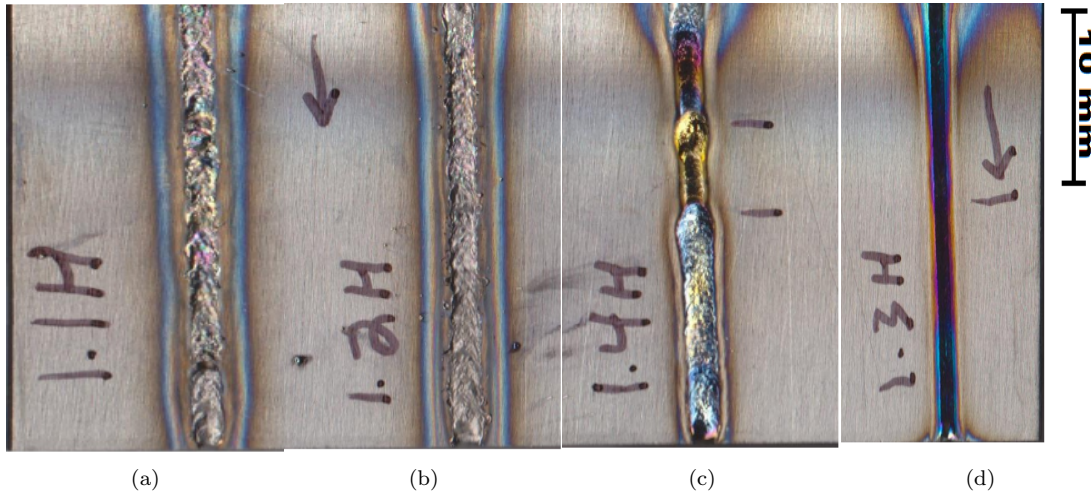


Figure 3.1: Varying off-focal distances on the Hf plate: (a) Laser focused on the surface of the plate; (b) Laser focused 2 mm above the surface; (c) Laser focused 4 mm above the surface; (d) Laser focused 8 mm above the surface of the plate. All scans were made at 90 mm/s.

### 3.1.2 Zirconium Coatings

Zirconium nitride, like hafnium nitride, has a golden color and the colors of zirconium oxide range from blue to black [4]. Figure 3.6 illustrates the effect of off-focal distance on the zirconium plate. As indicated in figure 3.6, scans 3.6c and 3.6d have a golden color which indicates the presence of zirconium nitride. (Note: The black appearance is an affect of the illumination conditions.) XRD results of scans 3.6c and 3.6d, shown in figures 3.7a and 3.8a indicated that less zirconium oxide was produced at an off-focal distance of 8 mm compared to 4 mm, at a translation speed of 90 mm/s. Scans 3.6a and 3.6b were gray-colored and irregular. As scans 3.6a and 3.6b were both consistent with melted zirconium, they were not analyzed using x-ray diffraction. The large peaks at 40 degrees in figures 3.7a and 3.8a were identified as zirconium nitride. The results from figures 3.7 and 3.8 indicated that an off-focal distance of 8 mm produced similar amounts of zirconium nitride to the off-focal distance of 4 mm at a translation speed of 90 mm/s.

A Philips XL30 environmental scanning electron microscope was used to characterize the zirconium nitride trail, produced at an off-focal distance of 8 mm and a scan speed of 90 mm/s, from figure 3.6d. An image of the trail at 50X magnification is shown in figure 3.9. This SEM image shows the smooth surface of the nitride trail as well as some cracks and light-gray features on the edges of the trails. A 250X magnification image, shown in figure 3.10, was then used to identify the light-gray features on the edges of the trail. To further understand the nature of the cracks, an image of a crack was taken at 2500X magnification in figure 3.11.

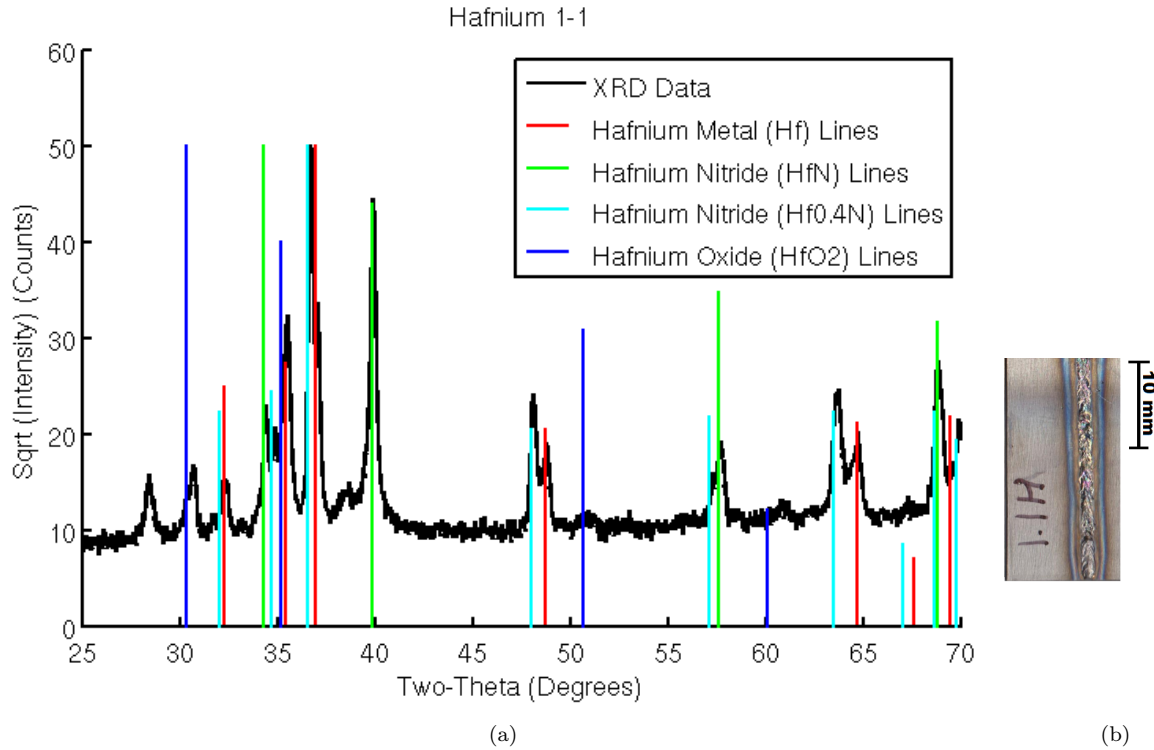


Figure 3.2: X-Ray diffraction analysis of trail 3.1a, showing a nitride film on hafnium and the presence of oxide.

### 3.2 Effect of Laser Scan Speed on Nitride Films

After analyzing the effects of the off-focal distance of laser-sustained plasma on hafnium and zirconium, different scan speeds were considered. An off-focal distance of 4 mm was chosen as a constant while the scan speed of the laser varied. For the hafnium samples, scan speeds of 20, 30, 40, and 75 mm/s were considered. A scan speed of 90 mm/s was previously tested when the off-focal distance was varied. An image of a scan from the 40 mm/s experiment is shown in figure 3.12. The trail in figure 3.12 was a dark green color which indicated that the coating had oxidized. The coatings produced at scan speeds of 30 mm/s and 50 mm/s also oxidized.

A cross section was taken from figure 3.1d, a trail produced at 90 mm/s scan speed at an OFD of 8 mm, to determine how much of the hafnium plate was affected by the laser. The cross section was cut and mounted in copper powder. After mounting the sample, the cross section was polished and etched with a solution consisting of 2 mL Hf, 9 mL  $\text{HNO}_3$ , and 9 mL  $\text{H}_2\text{O}$ . The cross section is shown in figure 3.13. The cross section revealed the convective flow lines of the nitride trail. A comparison was made to figure 3.14, taken from Nassar et al. [1], to show that similar flow lines also form during laser processing on titanium. The thickness of the trail varies from the outer lobes to the center of the trail. A measurement of the thickness of the outer lobe, produced at an off-focal distance of 8 mm and a scan speed of 90 mm/s, is shown in

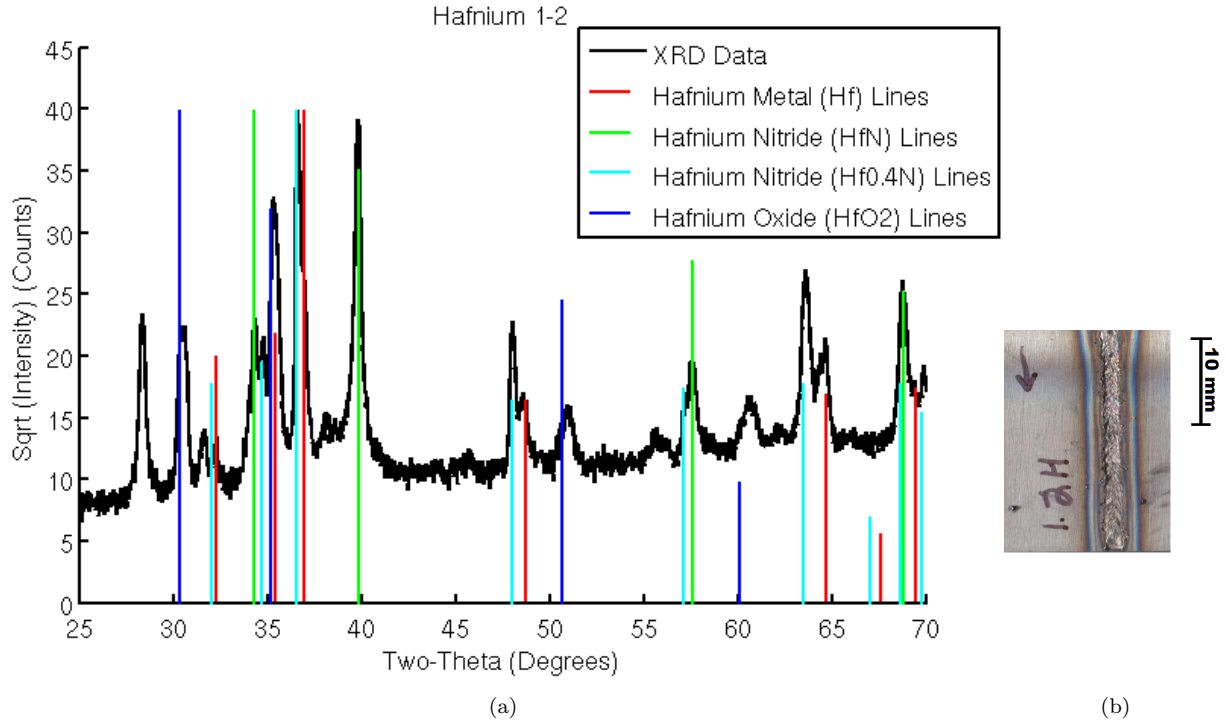


Figure 3.3: X-Ray diffraction analysis of trail 3.1b, OFD=2 mm, showing a nitride film on hafnium and more oxides.

figure 3.15 and a measurement of the thickness at the center of the same nitride trail is shown in figure 3.16. For the zirconium samples, a similar approach was used. Scan speeds of 10, 20, 30, 40, 50 and 75 mm/s were investigated. A scan speed of 90 mm/s was previously tested when off-focal distance was varied. Much like the hafnium coating, at 4 mm OFD and 40 mm/s, the zirconium coating was a smooth green film. As a result, higher speeds and larger off-focal distances were also explored.

The effect of a pre-struck laser-sustained plasma on a substrate during nitriding is not well understood [11]. To study this further, two scans were made at the same speed and off-focal distance. The results of these scans are shown in figure 3.17. Cross sections were taken from figures 3.17a and 3.17b to determine how a pre-struck plasma affected the nitriding process. The cross section was cut and mounted in copper powder. After mounting the sample, the cross section was polished and etched with a solution consisting of 10 mL Hf, 45 mL  $\text{HNO}_3$ , and 45 mL  $\text{H}_2\text{O}$ . The cross sections are shown in figures 3.18 and 3.19. The thickness of the trails were also measured. Figures 3.20 and 3.21 show the thickness of the outer lobe and center of the trail, produced at an off-focal distance of 8 mm and a scan speed of 90 mm/s without a pre-struck laser plasma without a pre-struck LSP, respectively. Figures 3.22 and 3.23 show the thickness of the outer lobe and center of the trail, produced at an off-focal distance of 8 mm and a scan speed of 90 mm/s with a pre-struck LSP, respectively indicating that the use of a pre-struck LSP in laser nitriding results in a thicker nitride trail. Data collected with a charge-coupled device (CCD)

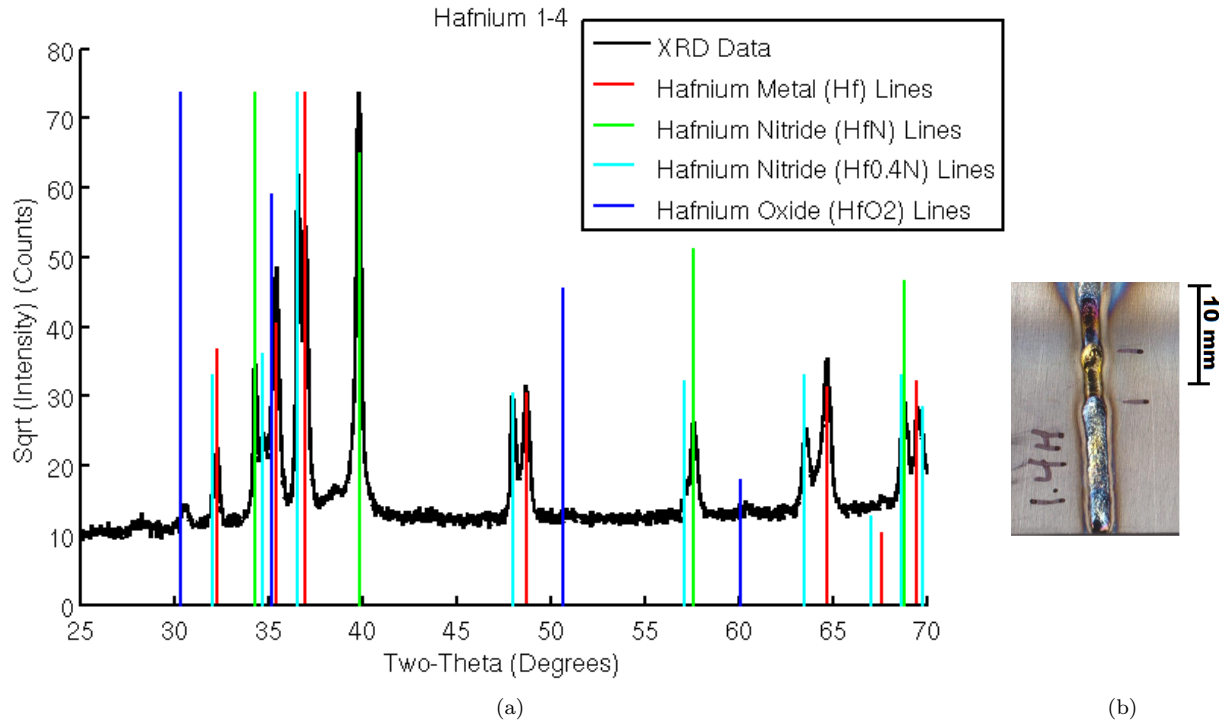


Figure 3.4: X-Ray diffraction analysis of trail 3.1c, OFD=4 mm, showing a nitride film on hafnium with minimal oxide.

revealed that at certain scan speeds and off-focal distances the plasma would be extinguished. This process can be seen in figure 3.24. The CCD also revealed that at other scan speeds and off-focal distances a laser-sustained plasma would form without being pre-struck. This process can be seen in figure 3.25.

### 3.3 Reproducibility of results

The parameters which were varied throughout the research were the off-focal distance and the translation speed of the substrate. The nitrogen gas flow and the laser power remained constant. It is necessary to reproduce this process given an optimal nitride range. In figure 3.8 the XRD data and consistency of the zirconium nitride film indicate that an off-focal distance of 8 mm and a translation speed of 90 mm/s will produce a useful nitride coating. The power measurements from that experiment showed that the laser was operating at 3.23 kW output power. The nitrogen flow around the laser cutting head was 10 L/min. To test the reproducibility of this process at a later date the laser was powered up to a power output of 3.25 kW and the nitrogen flow was again flowing at 10 L/min. A zirconium plate was scanned under the pre-struck laser-sustained plasma at an off-focal distance of 8 mm and a translation speed of 90 mm/s. The results indicated that this process was reproducible and a side-by-side comparison of the two scans can be seen in figure 3.26.

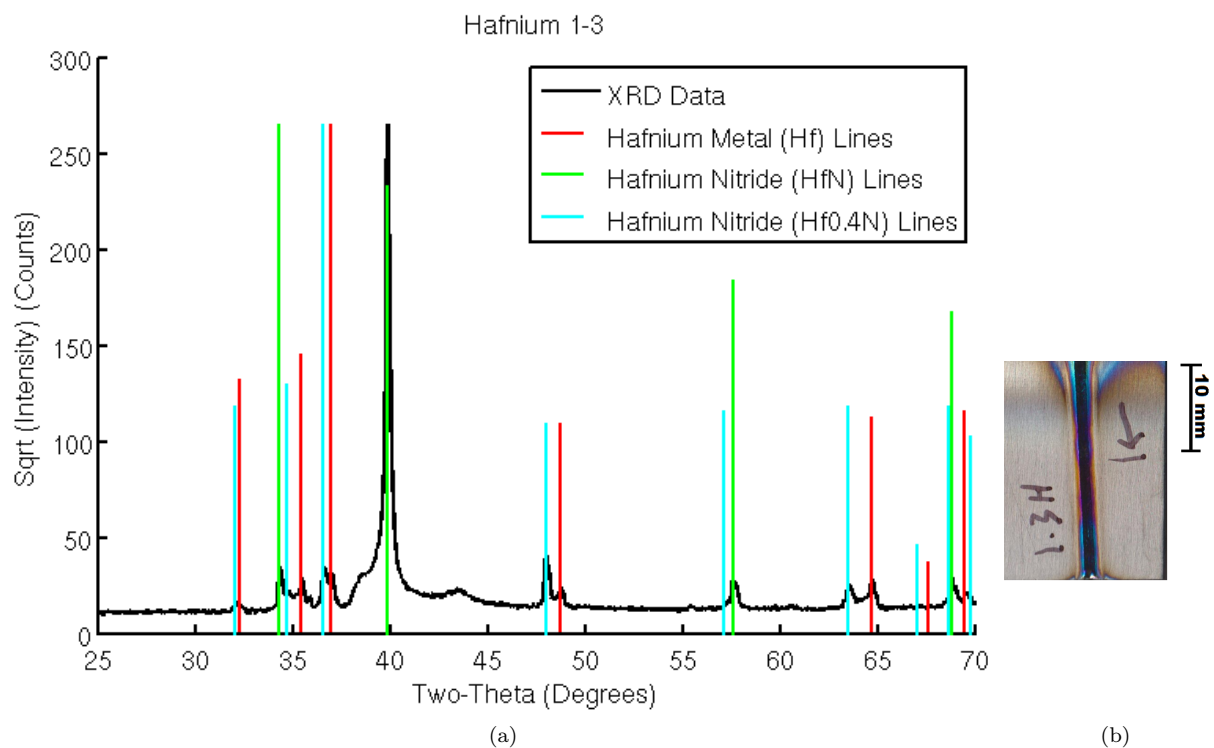


Figure 3.5: X-Ray diffraction analysis of trail 3.1d, OFD=8 mm, showing a nitride film on hafnium and no oxide present.

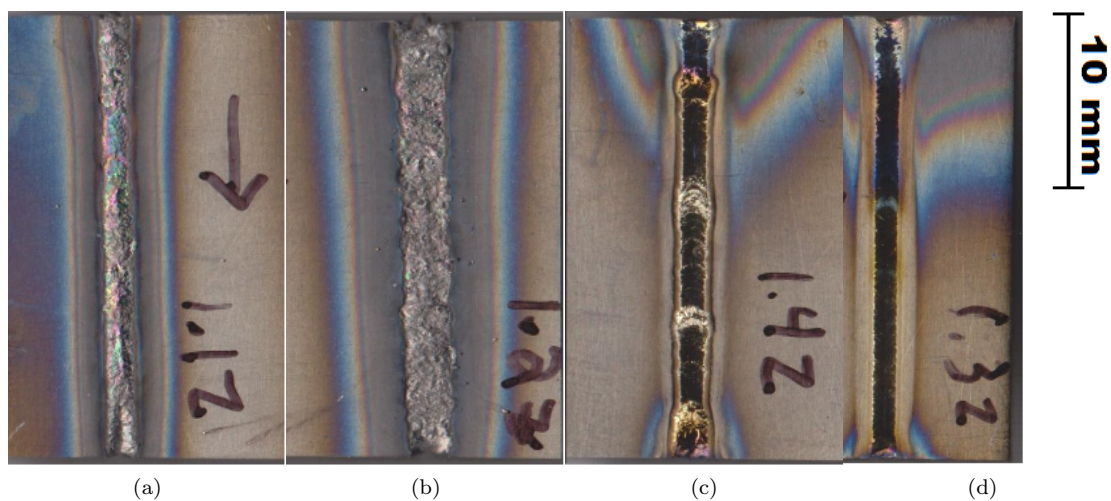


Figure 3.6: Varying off-focal distance on the Zr plate: (a) Laser focused on the surface of the plate; (b) Laser focused 2 mm above the surface; (c) Laser focused 4 mm above the surface; (d) Laser focused 8 mm above the surface of the plate. All scans were made at 90 mm/s.

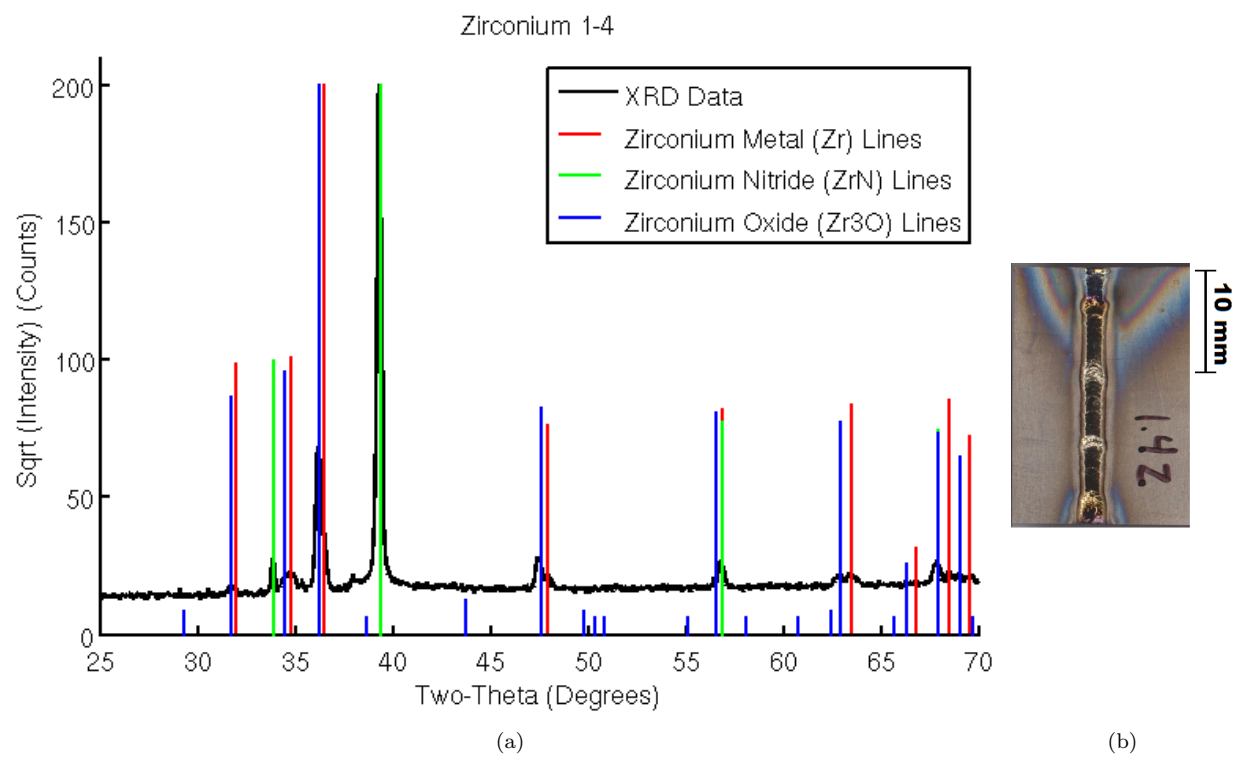


Figure 3.7: X-Ray diffraction analysis of trail 3.6c, OFD=4 mm, showing a nitride film on zirconium with minimal oxide present.

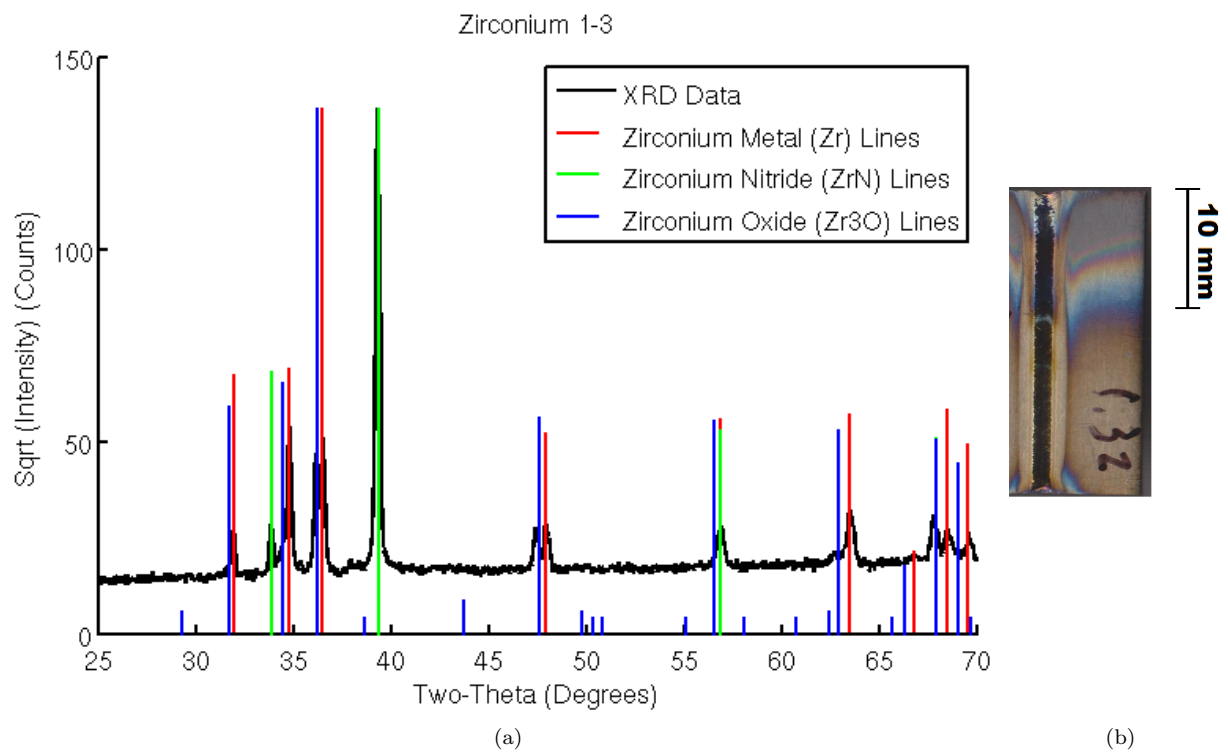


Figure 3.8: X-Ray diffraction analysis of trail 3.6d, OFD=8 mm, showing a nitride film on zirconium with an oxide present.



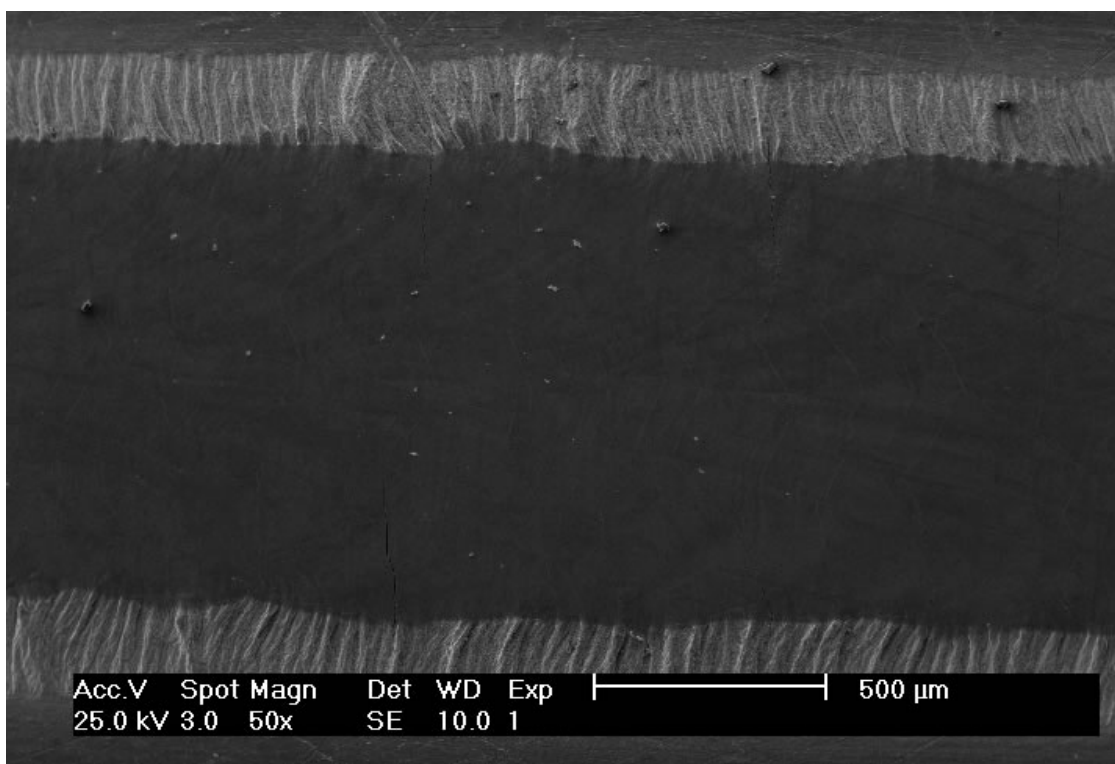


Figure 3.9: ESEM image of the zirconium nitride trail, produced at an off-focal distance of 8 mm and a scan speed of 90 mm/s, at 50X magnification.

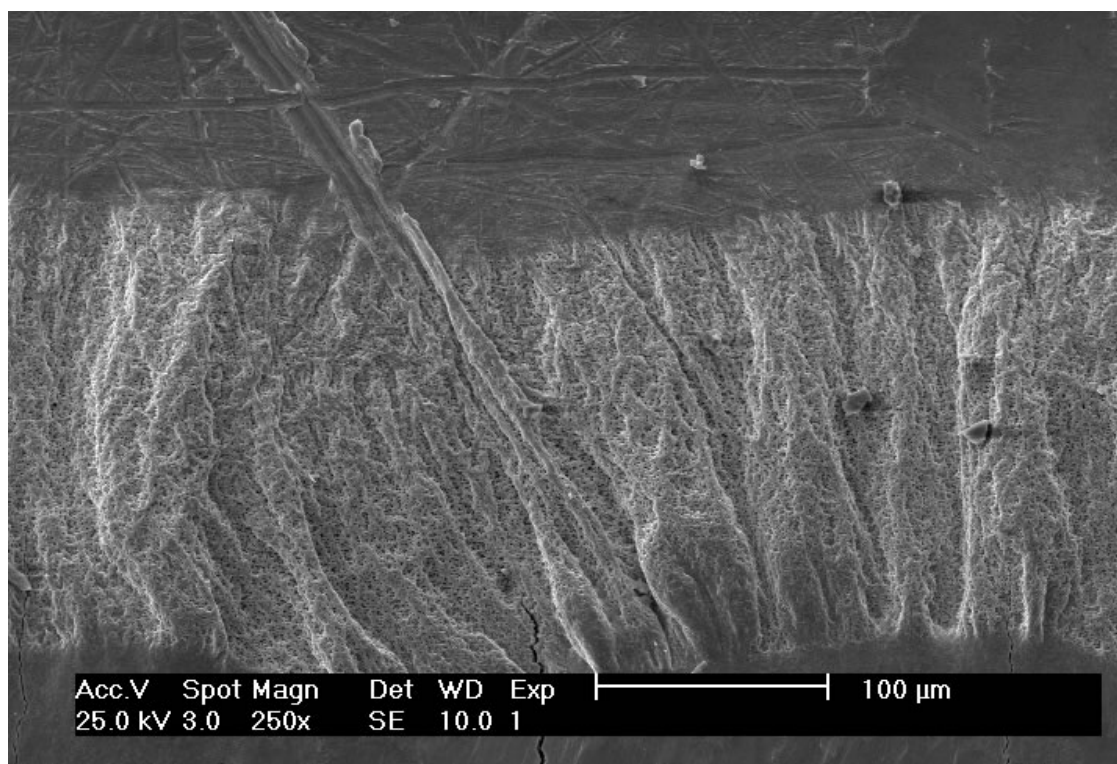


Figure 3.10: ESEM image of the zirconium nitride trail, produced at an off-focal distance of 8 mm and a scan speed of 90 mm/s, at 250X magnification.

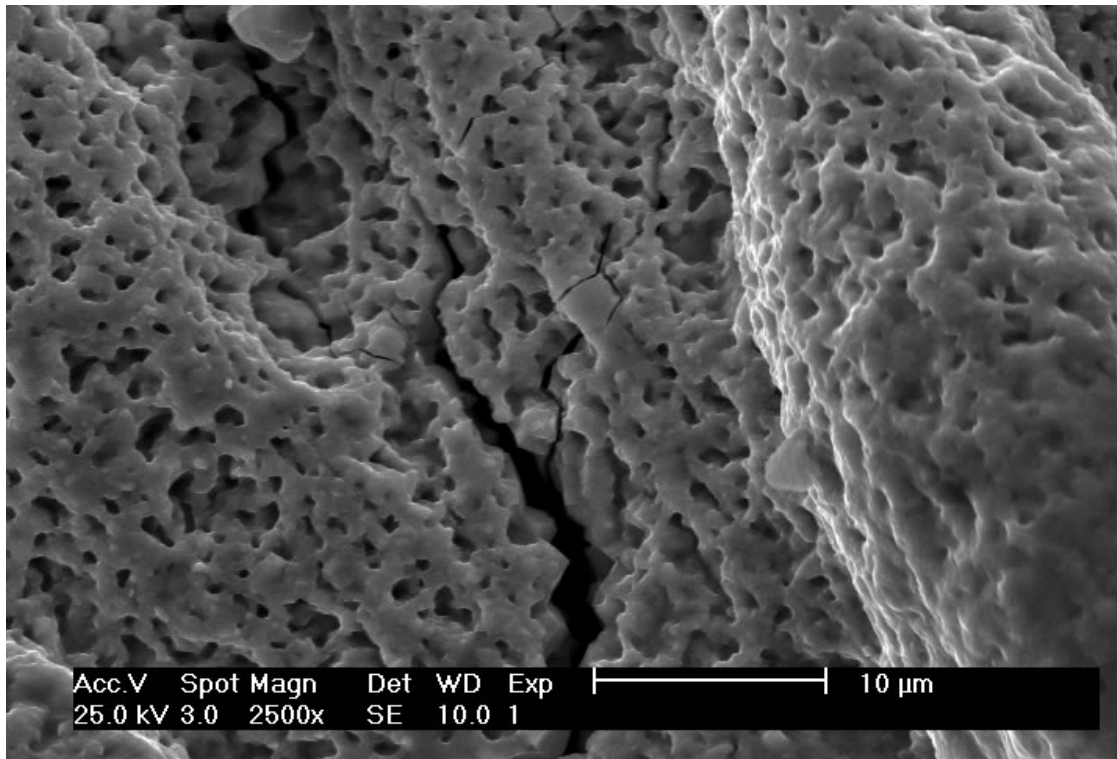


Figure 3.11: ESEM image of the zirconium nitride trail, produced at an off-focal distance of 8 mm and a scan speed of 90 mm/s, at 2500X magnification.

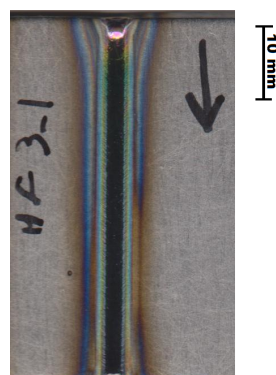


Figure 3.12: A scan produced by a pre-struck laser-sustained plasma at an off-focal distance of 4 mm and a scan speed of 40 mm/s.



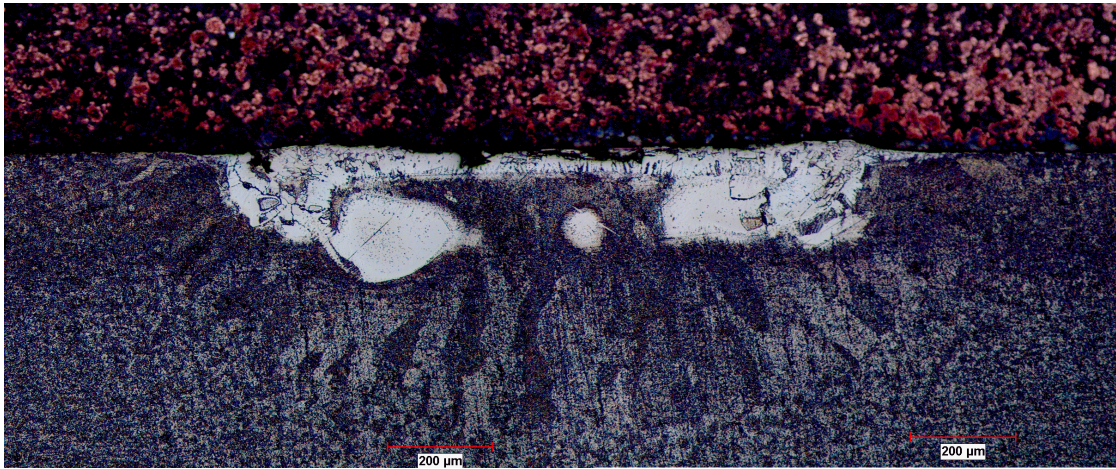


Figure 3.13: A cross section of a hafnium nitride scan produced at an off-focal distance of 8 mm and a scan speed of 90 mm/s.

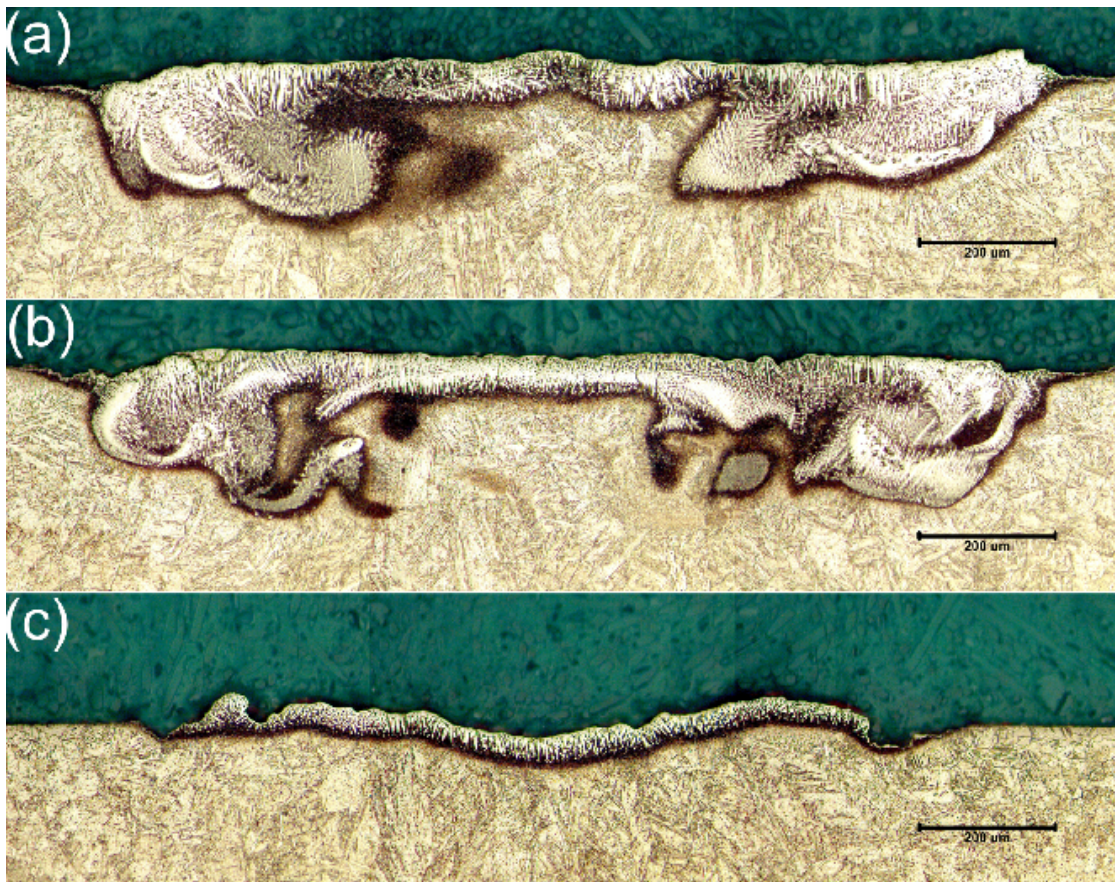


Figure 3.14: Cross-sectional images of the samples nitrided at 8 mm off-focus and 90 mm/s: (a) using a LSP; (b) without a LSP; and (c) using 1.9 kW output power, equal to the residual laser beam passing through the LSP. Image taken from Nassar et al. [1].



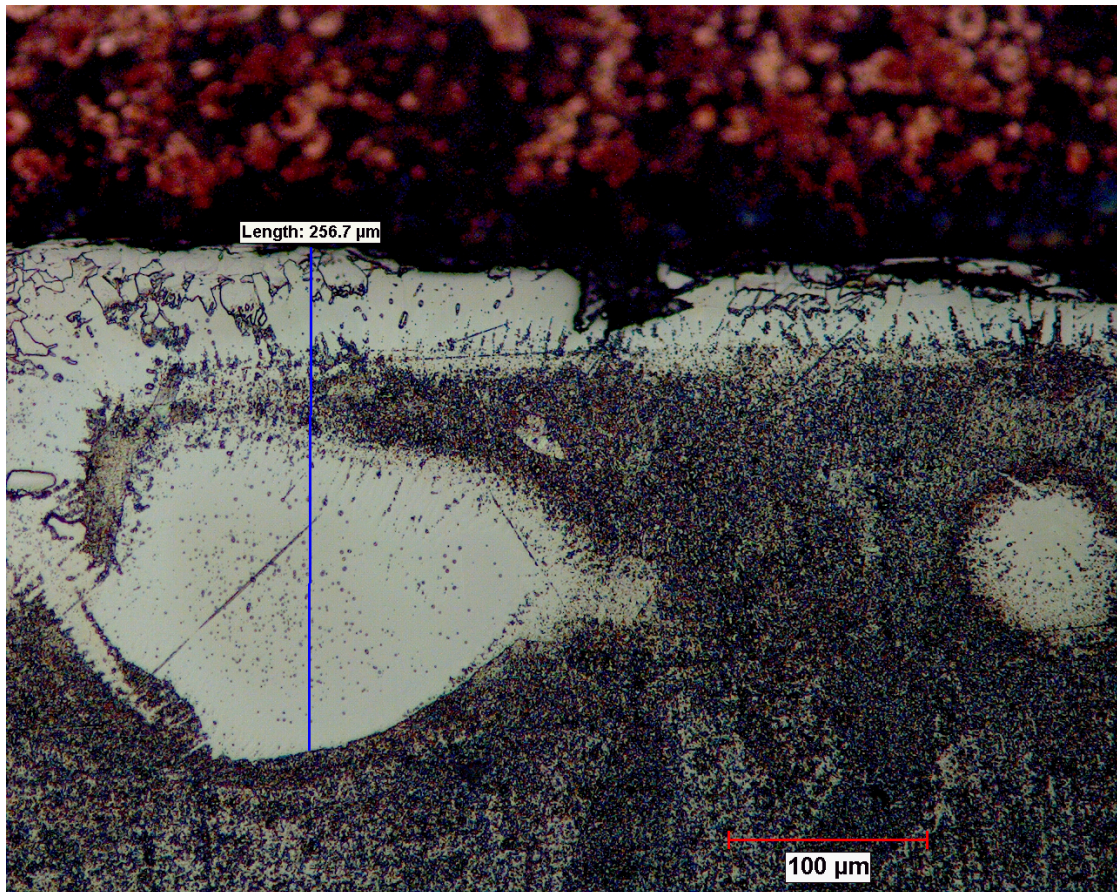


Figure 3.15: The thickness of the outer edge of the hafnium nitride trail, produced at an off-focal distance of 8 mm and a scan speed of 90 mm/s, is around 250 microns.



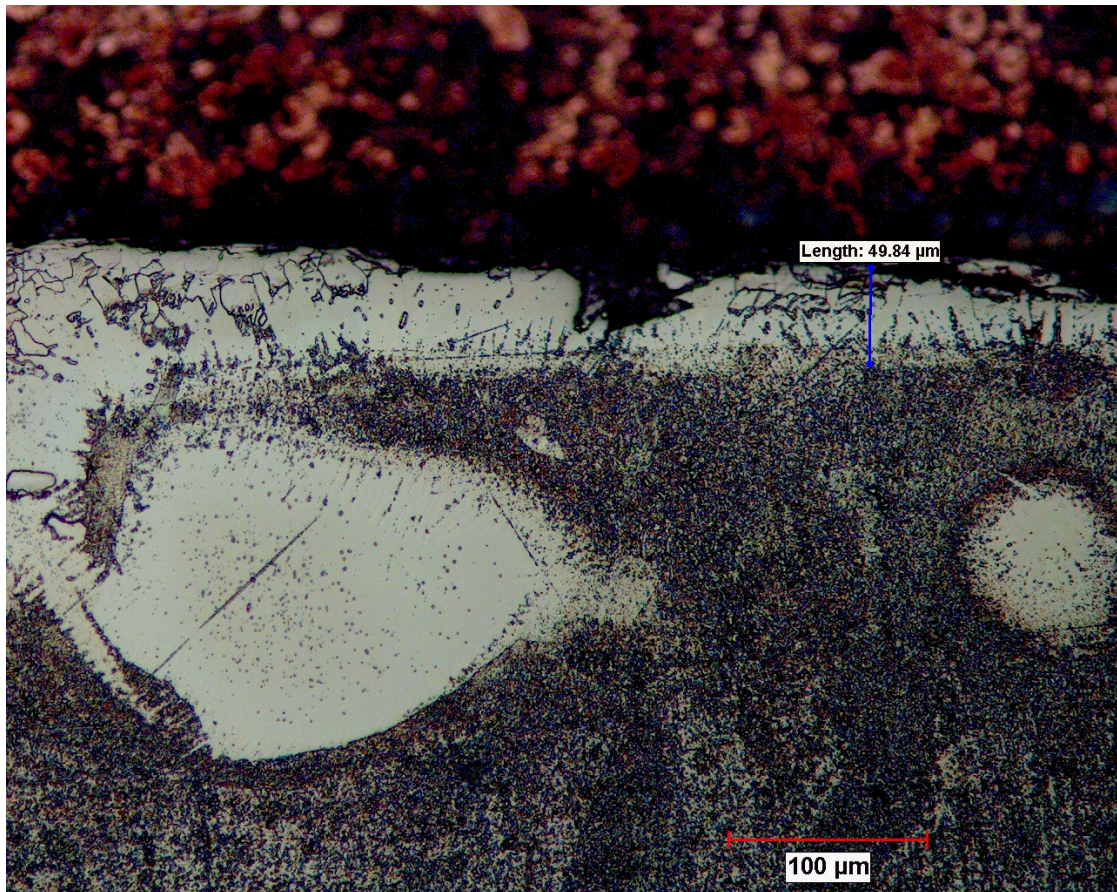


Figure 3.16: The thickness of the middle of the hafnium nitride trail, produced at an off-focal distance of 8 mm and a scan speed of 90 mm/s, is around 50 microns.

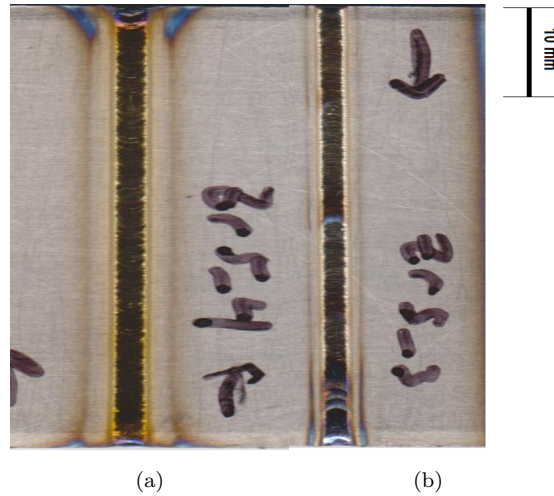


Figure 3.17: The effects of nitriding with a pre-struck laser-sustained plasma compared to nitriding without a pre-struck plasma: (a) Laser focused 8 mm above surface of the plate with a pre-struck laser-sustained plasma; (b) Laser focused 8 mm above the surface without a pre-struck plasma. All scans were made at 90 mm/s.

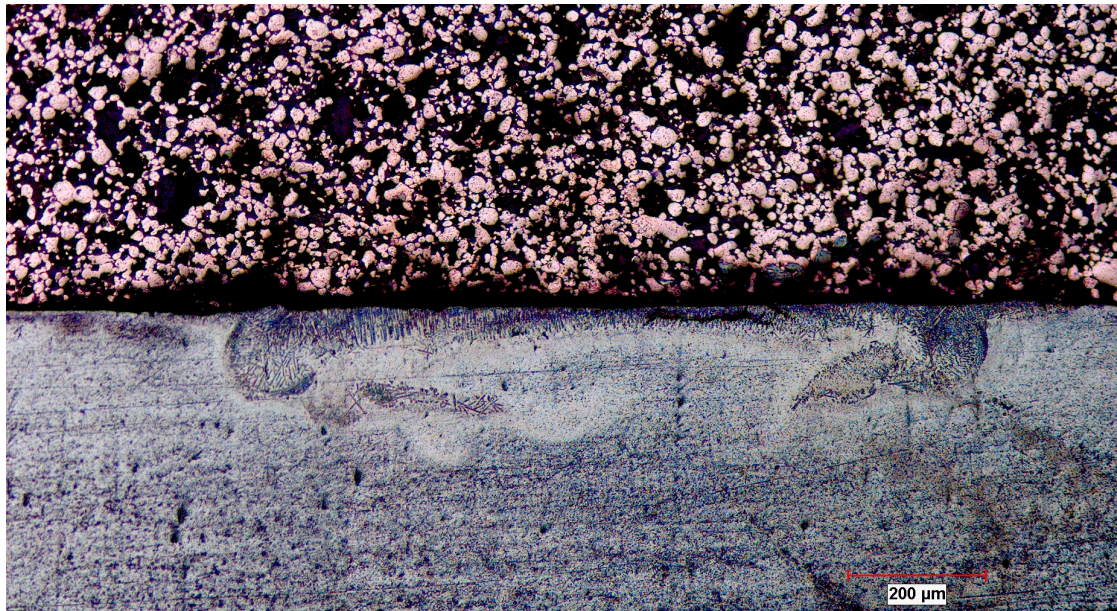


Figure 3.18: A cross section of a zirconium nitride scan produced at an off-focal distance of 8 mm and a scan speed of 90 mm/s without a pre-struck laser plasma.



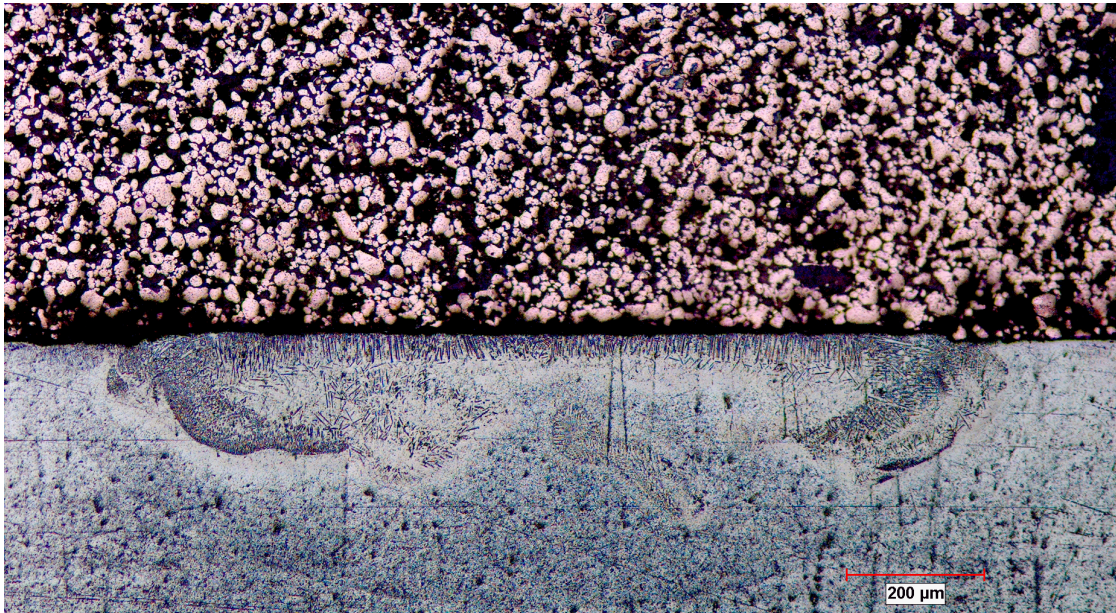


Figure 3.19: A cross section of a zirconium nitride scan produced at an off-focal distance of 8 mm and a scan speed of 90 mm/s with pre-struck laser-sustained plasma.



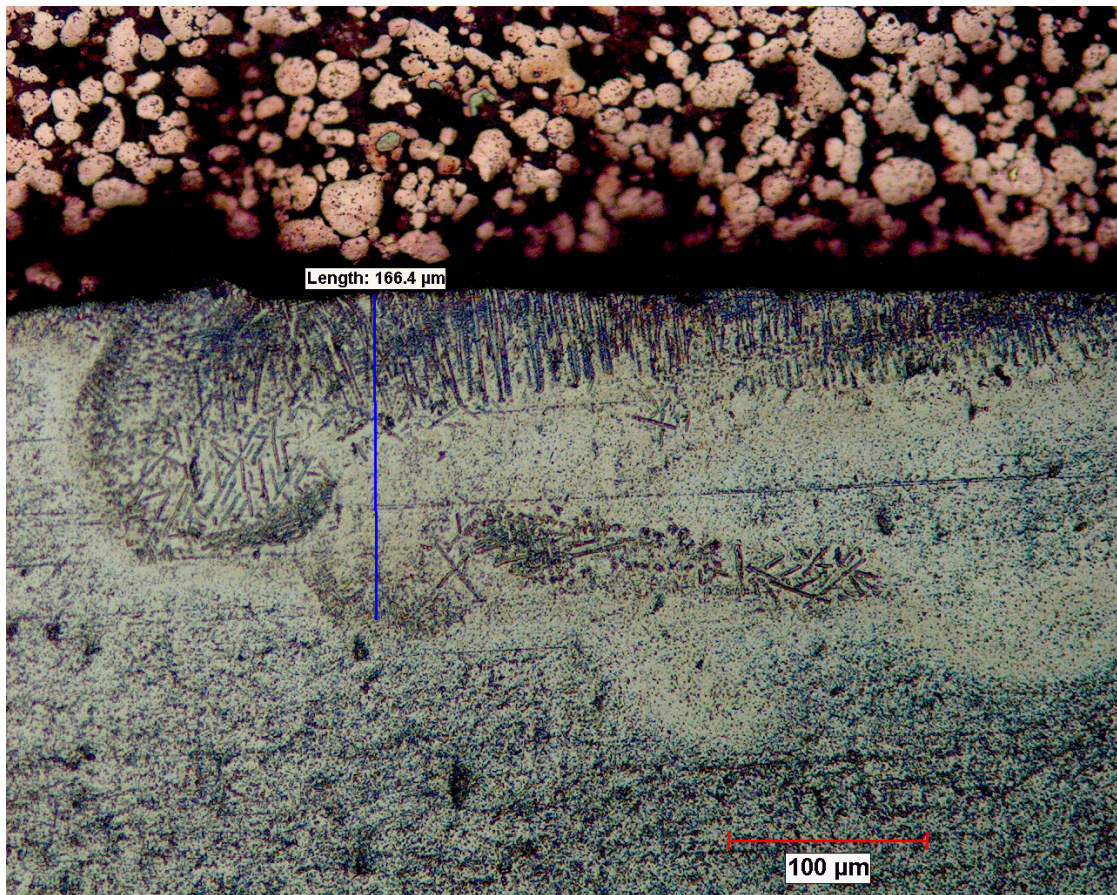


Figure 3.20: The thickness of the outer edge of the zirconium nitride trail, produced at an off-focal distance of 8 mm and a scan speed of 90 mm/s without a pre-struck laser, plasma is around 165 microns.



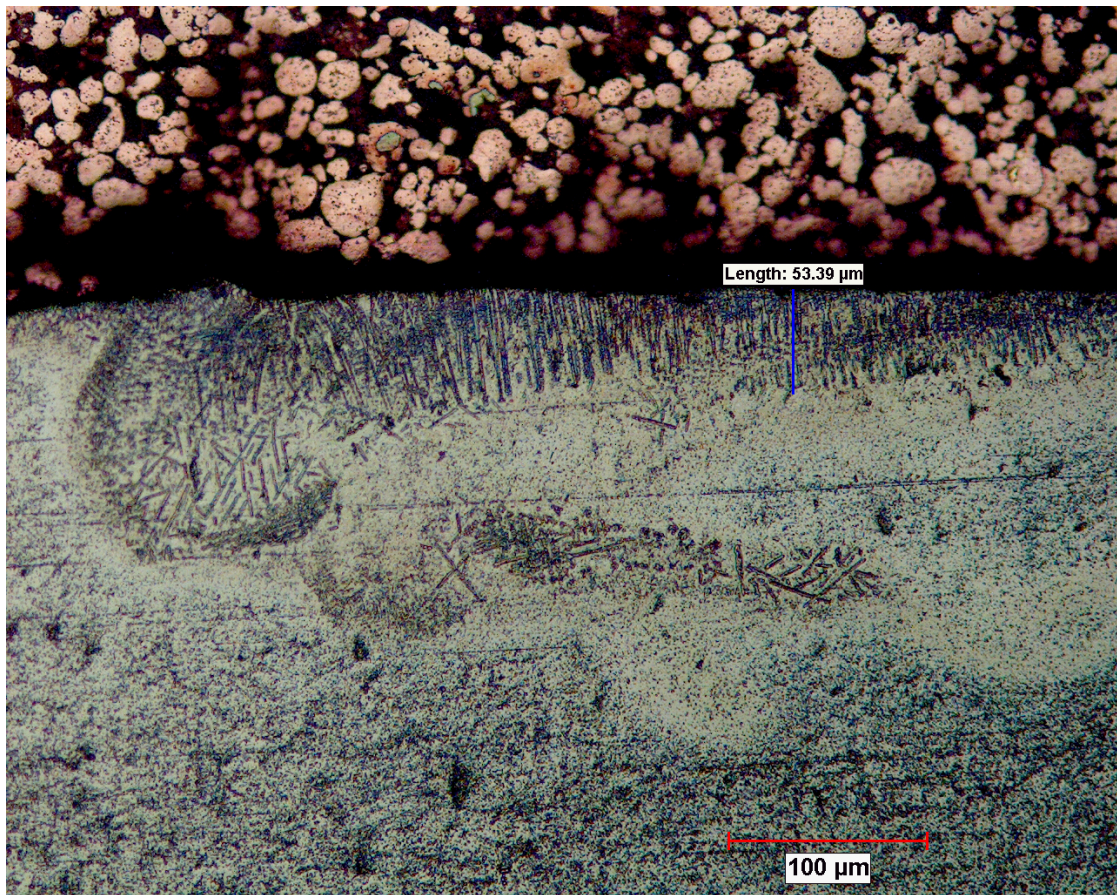


Figure 3.21: The thickness of the middle of the zirconium nitride trail, produced at an off-focal distance of 8 mm and a scan speed of 90 mm/s without a pre-struck laser plasma, is around 50 microns.



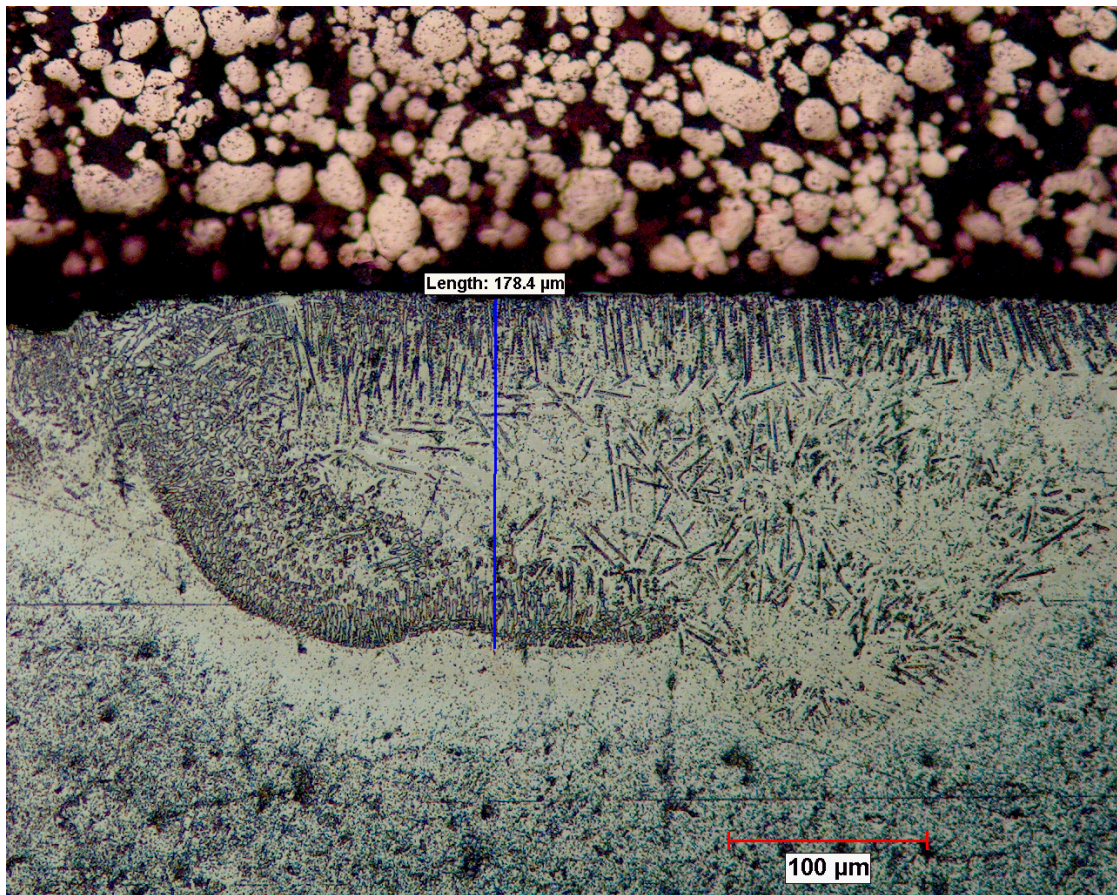


Figure 3.22: The thickness of the outer edge of the zirconium nitride trail, produced at an off-focal distance of 8 mm and a scan speed of 90 mm/s with pre-struck laser-sustained plasma, is around 180 microns.



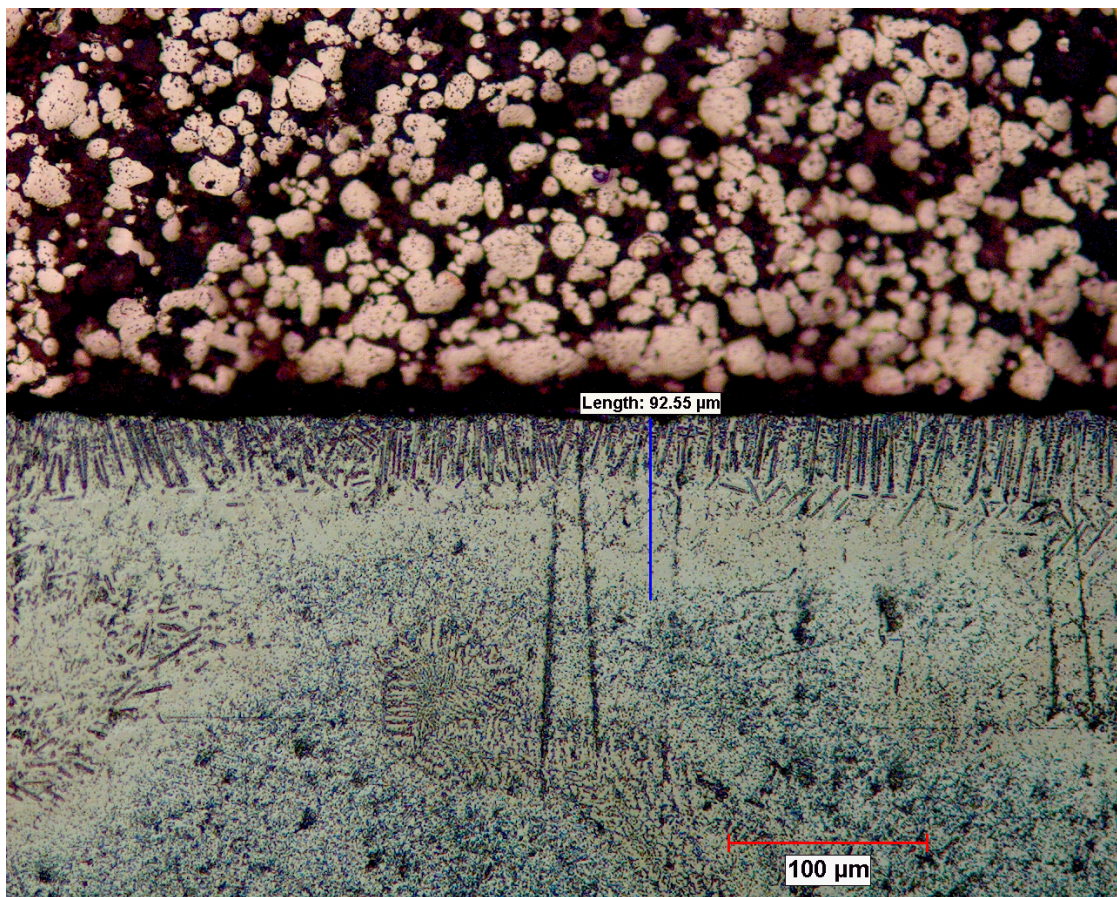


Figure 3.23: The thickness of the middle of the zirconium nitride trail, produced at an off-focal distance of 8 mm and a scan speed of 90 mm/s with pre-struck laser-sustained plasma, is around 90 microns.

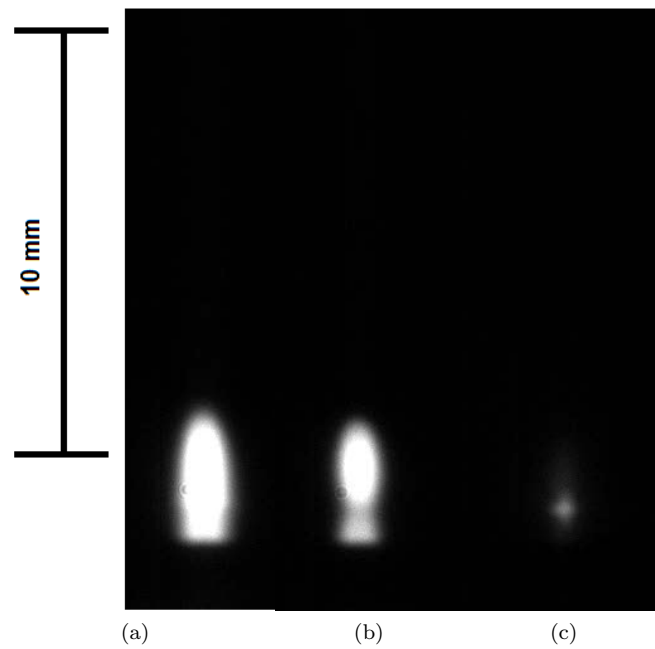


Figure 3.24: CCD images of plasma extinguishing while scanning a zirconium plate at the focal point of the laser: (a) the plasma touched the edge of the zirconium plate; (b) 0.005 seconds later the plasma begins to extinguish; (c) 0.01 seconds after the plasma touched the edge of the Zr plate it extinguished.

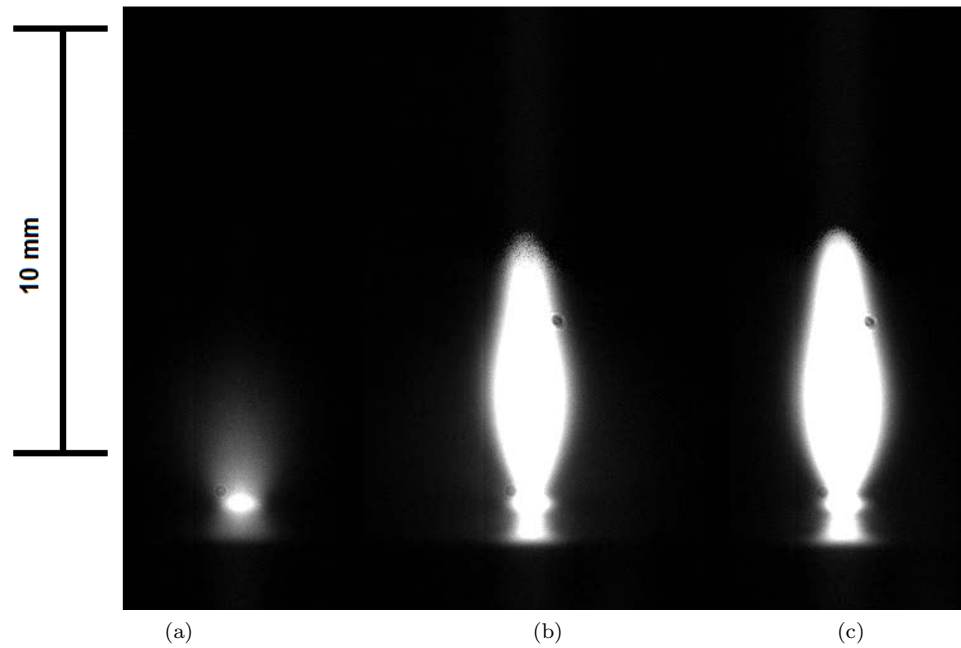


Figure 3.25: CCD images of a stable plasma igniting while scanning a zirconium plate at the an off-focal distance of 5mm and a translation speed of 90 mm/s: (a) the laser beam touched the edge of the zirconium plate; (b) 0.005 seconds later the plasma begins to ignite; (c) 0.005 seconds after the plasma ignited it appeared to be stable.

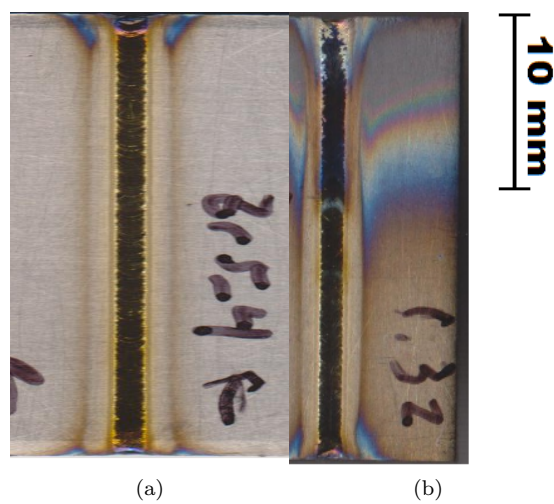


Figure 3.26: Two scans performed on separate Zr plates on different days with the same input parameters.

---

---

# CHAPTER 4

---

## DISCUSSION

### 4.1 Optimal Parameters for Nitride Film Production

When forming a nitride coating on a zirconium or hafnium substrate, some parameters yield more desirable results than others. From the XRD results of hafnium nitride coatings and from the observation of oxidized coatings a plot of scan speed versus off-focal distance was generated to identify regions that yielded near-stoichiometric coatings, as shown in figure 4.1. The laser scans which produced oxidized coatings or no coating at all are shown by red dots and listed as “No nitride formation.” The coatings which were golden yellow or confirmed as nitride coatings by XRD analyses are shown by dark blue dots and listed as “Nitride formed with plasma.” The two data points listed as possible nitride coatings were both a light green/yellow color and could not be classified without further analyses.

A more detailed parametric study was performed to determine the optimal range of zirconium nitride formation. This range is outlined in figure 4.2. There was a noticeable boundary dividing regions of zirconium nitride and zirconium oxide formation. As an oxidized nitride coating is undesirable, nitriding in the blue region is required to produce low-oxide coatings. For the parameters at which a zirconium nitride trail formed without a pre-struck laser-sustained plasma, a stable laser plasma formed during nitride processing. The CCD was able to capture the process of forming a stable plasma in figure 3.25. The use of a pre-struck laser-sustained plasma also increased the regions in which nitriding is possible.

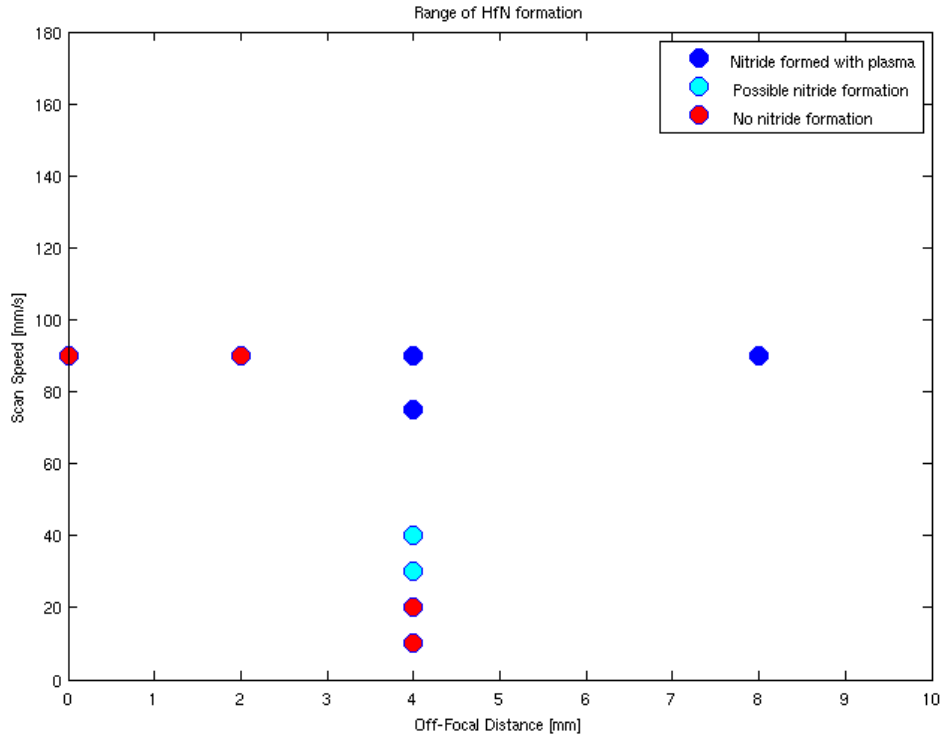


Figure 4.1: A plot of scan speed versus OFD, showing regions of hafnium nitride and oxidized coating formation.

## 4.2 The Role of a Laser-Sustained Plasma in Zirconium Nitride and Hafnium Nitride Production

For titanium substrates, it is known that the use of a pre-struck laser-sustained plasma expands the region in which nitriding is possible [1]. This research confirmed that this was also the case for laser-sustained plasma nitriding of hafnium and zirconium.

## 4.3 Other Effects of the Laser Nitriding Process

Although laser nitriding offers a rapid method for producing nitride coatings, some undesirable results were also noted. In figure 3.9 small cracks are visible near the edges of the nitride coating. A closer look at the edge of the trail can be seen in figure 3.10. The hollow structures on the edge of the nitride coating are believed to be partially decanted cellular dendrites [13]. Dendrites form when there is a temperature and concentration gradient in a material [14]. In this case, a concentration gradient between the molten zirconium and the highly energetic nitrogen plasma, was the most likely cause of dendrite formation. The excited nitrogen atoms are readily reacting with the molten zirconium and forming zirconium nitride. As the zirconium reacts near the



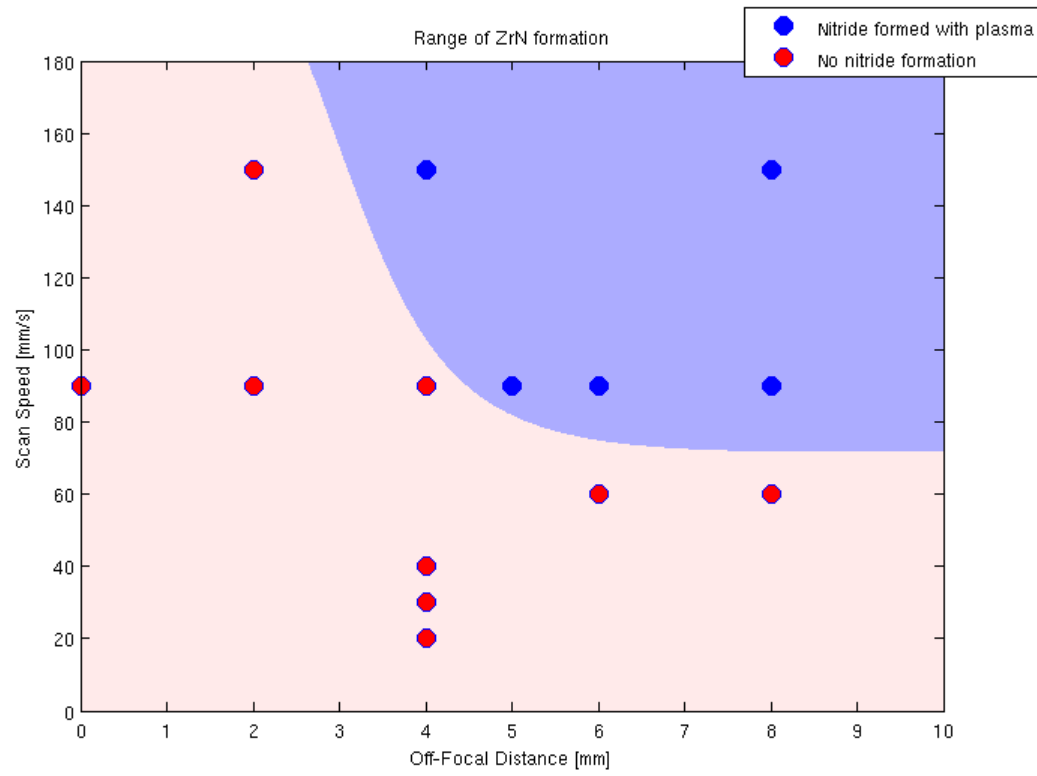


Figure 4.2: A plot of scan speed versus OFD, identifying regions of zirconium nitride and zirconium oxide formation.

middle of the trail, molten zirconium from the edges must be pulled in to satisfy the reaction. A closer look at a cellular dendrite can be seen in figure 3.11.

---

---

## CHAPTER 5

---

### CONCLUSIONS

Based on the experimental study of hafnium nitride and zirconium nitride formation using a laser-sustained nitrogen plasma, it was demonstrated that hafnium nitride and zirconium nitride coatings can be developed in open atmosphere. Regions of hafnium nitride and zirconium nitride formation, respectively, were identified as a function of LSP scan speed and off-focal distance.

Opportunities for future work include microstructural characterization, and optimization of the processing conditions for the development of defect-free, near-stoichiometric zirconium nitride and hafnium nitride coatings.

---

---

# APPENDIX A

---

## MATERIAL DATA

## FINE METALS CORPORATION

E-Mail: [finemetals@earthlink.net](mailto:finemetals@earthlink.net)  
[www.FineMetalsCorp.com](http://www.FineMetalsCorp.com)

15117 Washington Highway  
P. O. Box 1055 Ashland VA 23005

Phone: (804) 227-3381  
Fax: (804) 227-3404

**Certificate Of Analysis**

Customer: Penn State University

Material: Hafnium

Size: Thickness: 0.072 Inch Width: 1 Inch Length: 2 Inch

Qty/Unit: 6 Pieces

Lot Number: HF39550801

Temper:

P. O. #: E10-054972

Certification Of  
Conformance:

| Material(s) | Percentage |
|-------------|------------|
| Hafnium     | 99.95      |

| --- | Element    | --- | PPM | Percentage | Included                            | Method |
|-----|------------|-----|-----|------------|-------------------------------------|--------|
| Al  | Aluminum   | <   | 25  | 0.0025     | <input checked="" type="checkbox"/> |        |
| B   | Boron      | <   | 0.5 | 0.00005    | <input checked="" type="checkbox"/> |        |
| Bi  | Bismuth    | <   | 1   | 0.0001     | <input checked="" type="checkbox"/> |        |
| C   | Carbon     |     | 30  | 0.003      | <input type="checkbox"/>            |        |
| Cd  | Cadmium    | <   | 2.5 | 0.00025    | <input checked="" type="checkbox"/> |        |
| Co  | Cobalt     | <   | 5   | 0.0005     | <input checked="" type="checkbox"/> |        |
| Cr  | Chromium   | <   | 30  | 0.003      | <input checked="" type="checkbox"/> |        |
| Cu  | Copper     | <   | 20  | 0.002      | <input checked="" type="checkbox"/> |        |
| Fe  | Iron       |     | 155 | 0.0155     | <input checked="" type="checkbox"/> |        |
| Gd  | Gadolinium | <   | 3.5 | 0.00035    | <input checked="" type="checkbox"/> |        |
| H   | Hydrogen   | <   | 3   | 0.0003     | <input type="checkbox"/>            |        |
| Mn  | Manganese  | <   | 20  | 0.002      | <input checked="" type="checkbox"/> |        |
| Mo  | Molybdenum | <   | 10  | 0.001      | <input checked="" type="checkbox"/> |        |
| N   | Nitrogen   | <   | 20  | 0.002      | <input type="checkbox"/>            |        |
| Nb  | Niobium    | <   | 50  | 0.005      | <input checked="" type="checkbox"/> |        |
| Ni  | Nickel     | <   | 25  | 0.0025     | <input checked="" type="checkbox"/> |        |
| O   | Oxygen     |     | 190 | 0.019      | <input type="checkbox"/>            |        |
| P   | Phosphorus | <   | 3   | 0.0003     | <input type="checkbox"/>            |        |

\* I = Ion Interference C = Instrument Contamination S = Source Contamination

Lot Number: HF39550801

Date: 4/13/2011 9:47:41 AM

Hafnium

Page 1 of 2

Figure A.1: The material data sheet from Fine Metals Corp. detailing the purity of the samples used in this research. Page 1 of 3

| Certificate Of Analysis |             |   |       |           |                                     |
|-------------------------|-------------|---|-------|-----------|-------------------------------------|
| Pb                      | Lead        | < | 5     | 0.0005    | <input checked="" type="checkbox"/> |
| Si                      | Silicon     | < | 25    | 0.0025    | <input checked="" type="checkbox"/> |
| Sn                      | Tin         | < | 10    | 0.001     | <input checked="" type="checkbox"/> |
| Ta                      | Tantalum    | < | 1     | 0.0001    | <input checked="" type="checkbox"/> |
| Th                      | Thorium     | < | 3.5   | 0.00035   | <input checked="" type="checkbox"/> |
| Ti                      | Titanium    | < | 20    | 0.002     | <input checked="" type="checkbox"/> |
| U                       | Uranium     | < | 2     | 0.0002    | <input checked="" type="checkbox"/> |
| U-235                   | Uranium 235 | < | 0.007 | 0.0000007 | <input checked="" type="checkbox"/> |
| V                       | Vanadium    | < | 10    | 0.001     | <input checked="" type="checkbox"/> |
| W                       | Tungsten    | < | 20    | 0.002     | <input checked="" type="checkbox"/> |
| Zr                      | Zirconium   |   | 24200 | 2.42      | <input type="checkbox"/>            |

**Notes:**

This material cannot be rejected based on test results of another analytical laboratory alone. Test results may deviate from these values due to variations in each laboratory's testing methods. Any differences will be evaluated.

By: Thomas H. Goodloe  
Thomas H. Goodloe, Vice President

\* I = Ion Interference C = Instrument Contamination S = Source Contamination  
Lot Number: **HF39550801**

Date: 4/13/2011 9:47:41 AM **Hafnium** Page 2 of 2

Figure A.2: The material data sheet from Fine Metals Corp. detailing the purity of the samples used in this research. Page 2 of 3

# FINE METALS CORPORATION

15117 Washington Highway  
P. O. Box 1055 Ashland VA 23005

E-Mail: [finemetals@earthlink.net](mailto:finemetals@earthlink.net)  
[www.FineMetalsCorp.com](http://www.FineMetalsCorp.com)

Phone: (804) 227-3381  
Fax: (804) 227-3404

## Certificate Of Analysis

Customer: **Penn State University**

Material: **Zirconium 702**

Size: **Thickness: 0.08 Inch Width: 1 Inch Length: 2 Inch**

Qty/Unit: **6 Pieces**

Lot Number: **ZR298001XF1**

Temper:

P. O. #: **E10-054972**

Certification Of  
Conformance:

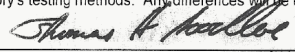
| Material(s)          | Percentage  |
|----------------------|-------------|
| <b>Zirconium 702</b> | <b>99.8</b> |

| ---   | Element       | --- | PPM   | Percentage | Included                            | Method |
|-------|---------------|-----|-------|------------|-------------------------------------|--------|
| C     | Carbon        |     | 500   | 0.05       | <input type="checkbox"/>            |        |
| Fe+Cr | Iron+Chromium |     | 2000  | 0.2        | <input checked="" type="checkbox"/> |        |
| H     | Hydrogen      |     | 50    | 0.005      | <input type="checkbox"/>            |        |
| Hf    | Hafnium       |     | 45000 | 4.5        | <input type="checkbox"/>            |        |
| N     | Nitrogen      |     | 250   | 0.025      | <input type="checkbox"/>            |        |
| O     | Oxygen        |     | 1600  | 0.16       | <input type="checkbox"/>            |        |

Notes: typical

This material cannot be rejected based on test results of another analytical laboratory alone. Test results may deviate from these values due to variations in each laboratory's testing methods. Any differences will be evaluated.

By:



Thomas H. Goodloe, Vice President

\* I = Ion Interference C = Instrument Contamination S = Source Contamination

Lot Number: **ZR298001XF1**

Date: 4/13/2011 9:49:24 AM

**Zirconium 702**

Page 1 of 1

Figure A.3: The material data sheet from Fine Metals Corp. detailing the purity of the samples used in this research. Page 3 of 3

---

# APPENDIX B

---

## MATLAB CODE

```
clear;clc
load Hf_Data_XRD.dat
twotheta=Hf_Data_XRD(:,1);
Hf1_1=Hf_Data_XRD(:,2);
Hf1_2=Hf_Data_XRD(:,3);
Hf1_3=Hf_Data_XRD(:,4);
Hf1_4=Hf_Data_XRD(:,5);
load Hf_Data_Lines.dat;
load Hf_Data_HfN_Lines.dat;
load Hf_Data_HfN_0_4_Lines.dat;
load Hf_Data_HfO2_Lines.dat;
hold on
%%%%%%%%%%%%%%%%%%%%%%%%%%%%%%%%%%%%%%%%%%%%%%%%%%%%%%%%%%%%%%%%%%%%%%%%
const1=max(Hf1_1)/max(Hf_Data_Lines(:,1));
const2=max(Hf1_1)/max(Hf_Data_HfN_Lines(:,1));
const3=max(Hf1_1)/max(Hf_Data_HfN_0_4_Lines(:,1));
const4=max(Hf1_1)/max(Hf_Data_HfO2_Lines(:,1));
plot(twotheta,sqrt(Hf1_1),'k','DisplayName','XRD Data')
stem(Hf_Data_Lines(:,2),sqrt(const1*Hf_Data_Lines(:,1)),'Marker','none','Color',
[1 0 0],'DisplayName','Hafnium Metal (Hf) Lines');
stem(Hf_Data_HfN_Lines(:,2),sqrt(const2*Hf_Data_HfN_Lines(:,1)),'Marker','none',
'LineStyle','-','Color',[0 1 0],'DisplayName','Hafnium Nitride (HfN) Lines');
stem(Hf_Data_HfN_0_4_Lines(:,2),sqrt(const3*Hf_Data_HfN_0_4_Lines(:,1)),
'Marker','none','LineStyle','-','Color',[0 1 1],'DisplayName','Hafnium Nitride
(Hf0.4N) Lines');
stem(Hf_Data_HfO2_Lines(:,2),sqrt(const4*Hf_Data_HfO2_Lines(:,1)),'Marker','none',
'LineStyle','-','Color',[0 0 1],'DisplayName','Hafnium Oxide (HfO2) Lines');
%%%%%%%%%%%%%%%%%%%%%%%%%%%%%%%%%%%%%%%%%%%%%%%%%%%%%%%%%%%%%%%%%%%%%%%%
xlabel('Two-Theta (Degrees)')
ylabel('Sqrt (Intensity) (Counts)')
title('Hafnium 1-1')
axis([25,70,0,60])
legend('show')
```

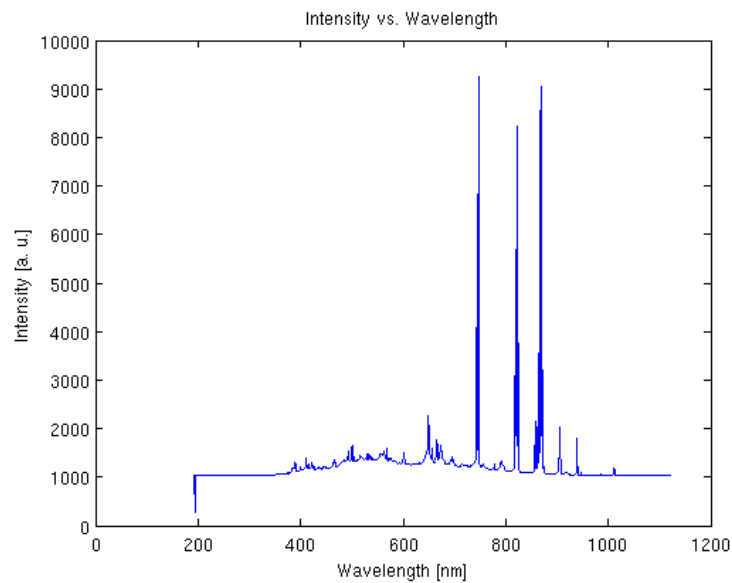
Figure B.1: Matlab Code used to produce XRD lines.

```

clear;clc
%The following code generates a contour plot to determine the time range to average
A=importdata('experiment2_hafnium.dat');
% contour(A,200)
% title('Contours of wavelength and intensity vs. Time')
% xlabel('Time [s]')
% ylabel('Contours of wavelength and intensity')
% average between 200 and 300
Wavelength=A(:,1);
Wavelength(1)=[]; %to delete info
Newdat=A(:,199:299);
Newdat(1,:)=[];
Meandat=mean(Newdat');
Final=[Wavelength Meandat'];
plot(Final(:,1),Final(:,2))
title('Intensity vs. Wavelength')
xlabel('Wavelength [nm]')
ylabel('Intensity [a. u.]')

%the next command saves the averaged data file to the correct file
%extension
save 06_23_11_N2_Hafnium_75mmps_4mmOFD_4msIT_ND0_6.dat Final -ASCII -tabs;

```



*Published with MATLAB® 7.10*

Figure B.2: Matlab Code used to produce averaged spectrum data.



---

# BIBLIOGRAPHY

- [1] NASSAR, A. R., R. AKARAPU, S. M. COPLEY, and J. A. TODD (Submitted: 2012) “Investigations of laser-sustained plasma and its role in laser nitriding of titanium,” *J. Phys. D: Appl. Phys.*, in submission to J. Phys. D: Appl. Phys.
- [2] URSU, I., I. N. MIHAILESCU, I. GUTU, A. HENING, T. JULEA, L. C. NISTOR, M. POPESCU, V. S. TEODORESCU, A. M. PROKHOROV, V. I. KONOV, and V. G. RALCHENKO (1986) “Surface nitridation of zirconium and hafnium by powerful cw CO2 laser irradiation in air,” *Appl. Opt.*, **25**(16), pp. 2720–2724.  
URL <http://ao.osa.org/abstract.cfm?URI=ao-25-16-2720>
- [3] TOTH, L. E. (1971) *Transition Metal Carbides and Nitrides*, Academic Press.
- [4] DAVIDSON, J. A. (1997), “Zirconium oxide and zirconium nitride coated stents,” .
- [5] PIERSON, H. O. (1996) *Handbook of Refractory Carbides and Nitrides: Properties, Characteristics, Processing, and Applications*, Noyes Publications.
- [6] SPROUL, W. D. (1984) “Hafnium nitride coatings prepared by very high rate reactive sputtering,” *Thin Solid Films*, **118**(3), pp. 279 – 284.  
URL <http://www.sciencedirect.com/science/article/pii/0040609084901986>
- [7] PICHON, L., T. GIRARDEAU, A. STRABONI, F. LIGNOU, J. PERRIRE, and J. FRIGRIO (1999) “Ion beam assisted deposition of zirconium nitrides for modulated optical index structures,” *Nuclear Instruments and Methods in Physics Research Section B: Beam Interactions with Materials and Atoms*, **147**(1-4), pp. 378 – 382.  
URL <http://www.sciencedirect.com/science/article/pii/S0168583X98005679>
- [8] RYKALIN, N. N. and A. A. UGLOV (1981) “Laser-plasma processing of metals at high gas pressures,” *Soviet Journal of Quantum Electronics*, **11**(6), p. 715.  
URL <http://stacks.iop.org/0049-1748/11/i=6/a=A05>
- [9] HÖCHE, D. and P. SCHAAF (2011) “Laser nitriding: investigations on the model system TiN. A review,” *Heat and Mass Transfer*, **47**, pp. 519–540, 10.1007/s00231-010-0742-z.  
URL <http://dx.doi.org/10.1007/s00231-010-0742-z>
- [10] URSU, I., I. N. MIHAILESCU, L. C. NISTOR, V. S. TEODORESCU, A. M. PROKHOROV, V. I. KONOV, and S. A. UGLOV (1987) “Multi-pulse laser nitridation of titanium, zirconium

and hafnium in a nitrogen atmosphere containing oxygen,” *Journal of Physics D: Applied Physics*, **20**(11), p. 1519.

URL <http://stacks.iop.org/0022-3727/20/i=11/a=025>

- [11] THOMANN, A., J. HERMANN, and C. BOULMER-LEBORGNE (1994) “TiN layer synthesis by laser-plasma,” *Thin Solid Films*, **241**, pp. 39 – 43, papers presented at the European Materials Research Society 1993 Spring Conference, Symposium C: Ion Beam, Plasma, Laser and Thermally-Stimulated Deposition Processes, Strasbourg, France, May , 1993.  
URL <http://www.sciencedirect.com/science/article/pii/0040609094903921>
- [12] SZYMANSKI, Z., Z. PERADZYNSKI, and J. KURZYNA (1994) “Free burning laser-sustained plasma in a forced flow,” *Journal of Physics D: Applied Physics*, **27**(10), p. 2074.  
URL <http://stacks.iop.org/0022-3727/27/i=10/a=014>
- [13] YILBAS, B. S., S. S. AKHTAR, and C. KARATAS (2012) “Laser gas assisted nitriding of Hastelloy G Alloy: thermal stress analysis and characterization,” *Surface and Interface Analysis*, **44**(3), pp. 352–364.  
URL <http://dx.doi.org/10.1002/sia.3811>
- [14] M.E. and GLICKSMAN (1984) “Free dendritic growth,” *Materials Science and Engineering*, **65**(1), pp. 45 – 55, solidification Microstructure: 30 Years after Constitutional Supercooling.  
URL <http://www.sciencedirect.com/science/article/pii/0025541684901988>

## Curriculum Vitae

**TIMMY STRAIT**

Timmy L. Strait III  
(717) 504-5722  
txs345@psu.edu  
2320 Plaza Drive  
State College, PA 16801

### EDUCATION

The Pennsylvania State University, University Park, PA:

- Bachelor of Science in Engineering Science; Honors curriculum
- Minor in Math and Physics

Graduation:

Spring 2012

- Master of Science in Engineering Science and Mechanics

Graduation:

Spring 2013

Honors Programs:

- Penn State University Schreyer Honors College
- Penn State University Deans List
- Penn State University Mont Alto Campus Honors Program

Fall 2010-Current

Fall 2008-Fall 2010

Fall 2008-Fall 2010

### WORK EXPERIENCE

Penn State College of Engineering, University Park, PA:

May 2011-Current

- Researched the application of laser plasma in material science and manufacturing while working with a Class IV laser.

Penn State Creamery, University Park, PA:

Jan. 2011-Current

- Worked as a cashier and served customers.

Penn State Academic Support Center, Mont Alto, PA:

Jan. 2009-May 2010

- Provided peer tutoring and instruction for various courses including chemistry, economics, and thermodynamics.
- Received level 2 certification from the CRLA.

McDonalds Corp., McConnellsburg, PA:

May 2008-June 2010

- Worked as a cashier, food assembler, and custodian.

### ACTIVITIES

Penn State University Mont Alto Research Program:

- Researched and developed the bio-diesel project which converted waste vegetable oil into usable bio-fuels.
- Experimentally collected musical waveforms and analyzed frequencies to determine the properties of the instruments.

Aug. 2008-Feb. 2009

Jan. 2009-April 2009

Penn State Academic Festival:

Fall 2009-Spring 2010

- Submitted a solid state Tesla coil along with other research projects into the academic fair.